Pax3 Expression in Satellite Cells of Avian Skeletal Muscle Spindles during Normal Development and with Experimental Muscle Overload

A thesis submitted to the College of Graduate Studies and Research in partial fulfillment of the requirements for the degree of Master of Science in the Department of Anatomy and Cell Biology at the University of Saskatchewan

By

Lisa Janelle Kirkpatrick

Permission To Use

In presenting this thesis in partial fulfillment of the requirements for a Master of Science degree from the University of Saskatchewan, I agree that the libraries of this University may make it freely available for inspection. I further agree that permission for copying of this thesis in any manner, in whole or in part, for scholarly purposes may be granted by professors who supervised my thesis work or, in their absence, by the Head of the Department or the Dean of the College in which my thesis work was done. It is also understood that any copying or publication or use of this thesis or parts there of for financial gain shall not be allowed without my written permission. It is also understood that due recognition shall be given to me and to the University of Saskatchewan in any scholarly use which may be made of any materials in my thesis.

Requests for permission to copy or to make other use of material in this thesis in whole or part should be addressed to:

Head of the Department of Anatomy and Cell Biology
University of Saskatchewan
107 Wiggins Road
Saskatoon, Saskatchewan S7N 5E5
CANADA

Abstract

Pax3 protein is initially expressed in the dermomyotome of embryonic somites, which gives rise to skeletal muscle. Following myogenesis, Pax3 expression is mostly down-regulated and becomes restricted to a few satellite cells (SCs) of select mature muscles. SCs are activated to form new myonuclei during muscle hypertrophy, regeneration and repair. Intrafusal fibers of muscle spindles are thought to persist in a comparatively immature state as, unlike extrafusal fibers, they maintain small diameters, developmental myosins, Myf5 expression and high SC concentrations. This thesis tests the hypotheses that Pax3 expression is preferentially maintained in SCs of adult skeletal muscle spindles and can be augmented under conditions of SC activation. To study Pax3 through development, immunohistochemical techniques were used to identify SCs by their Pax7 expression, and analyze the proportion of SCs and myonuclei (MN) expressing Pax3 in chicken anterior latissimus dorsi (ALD) muscle excised at 9, 30, 62, and 145 days post-hatch. To induce SC activation, tenotomy was performed on the right ALD muscle of 138-day post-hatch chicks to induce compensatory hypertrophy of the ipsilateral synergistic posterior latissimus dorsi (PLD) muscle. The PLD was analyzed seven days after ALD tenotomy using similar immunohistochemical techniques. This is the first study to show Pax3-expressing SCs within intrafusal fibers of muscle spindles. This thesis demonstrates that throughout development there is a higher percentage of Pax3-expressing SCs within intrafusal fibers of muscle spindles than the surrounding extrafusal fibers that compose the bulk of the muscle. It is also revealed that the proportion of the SC population expressing Pax3 declines with age in both intrafusal and extrafusal fibers. Compensatory hypertrophy of the PLD resulted in a greater percentage

of Pax3-expressing SCs in intrafusal and extrafusal fibers than under control conditions. The percentage of SCs expressing Pax3 after PLD overload was similar to that seen in young control muscle. The percentage of Pax3-expressing MN also increased after muscle overload to levels seen in young muscle. A disproportionate decrease in the proportion of SCs expressing Pax3 during development, and a disproportionate increase in the percentage of Pax3 positive SCs as a result of experimentally induced muscle hypertrophy, suggests that Pax3 expression in maturing muscle may be more than just a developmental vestige. Pax3 may be a factor in the activation and differentiation of SCs in maturing muscle.

Acknowledgements

First and foremost, I would like to thank my supervisor Dr. Benjamin W.C. Rosser for taking a chance on a prospective undergraduate summer student, and molding me into the graduate student I am today. I would not have achieved the successes I have without his guidance, encouragement, expertise and generosity throughout my entire time under his supervision.

I wish to thank my co-supervisor Dr. Helen Nichol for all the opportunities and guidance she provided me along the way, and for finding a place for me in her active laboratory and busy schedule.

Thanks to the members of my Advisory Committee, Dr. William Kulyk and Dr. Patrick Krone, for their valuable time and guidance throughout this process. Thanks also to my external examiner, Dr. Adil Nazarali (College of Pharmacy and Nutrition, University of Saskatchewan), for taking the time to participate in my thesis defense.

A special thanks to Dr. Zipora Yablonka-Reuveni (Department of Biological Structure, School of Medicine, University of Washington) for her excellent advice and friendly hospitality throughout my time as a graduate student, and to Dr. Everett Bandman (Department of Food Sciences and Technology, University of California) for his gift of the monoclonal NA4 antibody. A. Kawakami and C.P. Ordahl, respectively, developed antibodies against Pax7 and Pax3, obtained from the Developmental Studies

Hybridoma Bank developed under the auspices of the NICHD and maintained by the University of Iowa, Department of Biological Sciences, Iowa City, IA 52242.

I would like to thank those members of the Department of Anatomy and Cell Biology who were particularly helpful throughout the completion my research: Karen Yuen, Tonya McGowan, Shirley West, Corrine Howells, and Cynthia Kovacs.

Thank you to my parents and brother for all their support and words of encouragement throughout the years. This thesis is the all-encompassing answer to that question I was asked so often: "So what exactly are you studying?"

Finally, to Lee Connell, thank you for keeping me sane throughout this process. Your love and support have meant the world to me and I really could not have done this without you. You're the best.

An Alexander Graham Bell Graduate Scholarship from the Natural Sciences and Engineering Research Council of Canada (NSERC) provided funding for my studies. A Discovery Grant awarded to Dr. Benjamin W.C. Rosser from NSERC provided funds for this thesis. Additional funds were provided by the College of Medicine, University of Saskatchewan.

Table of Contents

Permission To Use I

Abstract II

Acknowledgements IV

Table of Contents VI

List of Tables VIII

List of Figures IX

List of Abbreviations XI

Chapter 1: General Introduction 1

Chapter 2: Specific Aims 16

Chapter 3: Pax3 Expression in Satellite Cells of Post-Hatch Muscle Spindles . . . 18

3.1 Abstract 19

3.2 Introduction 20

3.3 Materials and Methods. 23

3.3.1 Experimental Model 23

3.3.2 Tissue Preparation and Sectioning 23

3.3.3 Immunohistochemistry 24

3.3.4 Imaging and Analysis 26

3.3.5 Statistics 28

3.4 Results 29

3.4.1 Identifying Structures 29

3.4.2 Anterior Latissimus Dorsi Muscle Weight 29

3.4.3 Ellipse Minor Axis 36

3.4.4 Satellite Cell Frequency 36
3.4.5 Satellite Cells Expressing Pax3 39
3.4.6 Myonuclei Expressing Pax3 40
3.5 Discussion 41
Chapter 4: Pax3 Expression Increases with Muscle Overload 45
4.1 Abstract 46
4.2 Introduction 47
4.3 Materials and Methods 51
4.3.1 Experimental Model 51
4.3.2 Tissue Preparation and Sectioning 52
4.3.3 Immunohistochemistry 52
4.3.4 Imaging and Analysis 54
4.3.5 Statistics 55
4.4 Results 57
4.4.1 Identifying Structures 57
4.4.2 Posterior Latissimus Dorsi Muscle Weight 57
4.4.3 Ellipse Minor Axis 62
4.4.4 Satellite Cell Frequency 63
4.4.5 Satellite Cells Expressing Pax3 67
4.4.6 Myonuclei Expressing Pax3 68
4.5 Discussion 69
Chapter 5: General Discussion 74
Literature Cited 80

List of Tables

Chapter 1:

Table 1: Pax gene expression profile and associated human diseases 6

Chapter 3:

Table 2: Primary and secondary antibodies and corresponding structure labeled 25

List of Figures

Chapter 1:

Figure 1: Dermomyotome and myotome of a mouse thoracic embryonic somite at approximately E9-10 3

Figure 2: Satellite cell and myonuclei within a skeletal muscle fiber 8

Figure 3: Muscle spindle within avian skeletal muscle 11

Figure 4: Dorsal view of the right side of the avian thorax and proximal wing, showing the anterior and posterior latissimus dorsi muscles 14

Chapter 3:

Figure 5: Immunohistochemical labeling of serial cross-sections of anterior latissimus dorsi muscle at 9 and 30 days post-hatch 30

Figure 6: Immunohistochemical labeling of serial cross-sections of anterior latissimus dorsi muscle at 62 and 145 days post-hatch 32

Figure 7: Anterior latissimus dorsi muscle weight and fiber size data 34

Figure 8: Anterior latissimus dorsi muscle intrafusal and extrafusal fiber nuclei data 37

Chapter 4:

Figure 9: Immunohistochemical labeling of serial cross-sections of posterior latissimus dorsi muscle in 30 day, mature control and mature experimental post-hatch muscle 58

Figure 10: Posterior latissimus dorsi muscle weight and fiber size data 60

Figure 11: Histogram of ellipse minor axis of extrafusal fibers in posterior latissimus dorsi muscle 64

Figure 12: Posterior latissimus dorsi muscle intrafusal and extrafusal nuclei data 65

List of Abbreviations

ALD	anterior latissimus dorsi
BCL-XL	B-cell lymphoma – extra large
DM	dermomyotome
EDTA	ethylenediaminetetraacetic acid
MN	myonuclei
MRF	myogenic regulatory factor
Pax3	paired box transcription factor three
Pax7	paired box transcription factor seven
PBS	phosphate buffer saline
PLD	posterior latissimus dorsi
RT-PCR	reverse transcription polymerase chain reaction
SC	satellite cell
SCN	satellite cell nuclei
SE	standard error
%MN Pax3+	percentage of myonuclei expressing Pax3
%SC Pax3+	percentage of satellite cells expressing Pax3

Chapter 1:

General Introduction

Skeletal muscle tissue is found in many functional compartments throughout the body. Approximately 700 individual muscles constitute about 40% of total body weight in adult humans. This can be a greater percentage of body weight in other vertebrates. Skeletal muscle performs a wide variety of functions, including movement (locomotion, breathing, mastication, vocalization, facial expression, eye movement, swallowing) postural maintenance, thermogenesis and protein reserve. All but the latter are dependent upon muscle contraction.

The contractile cellular unit of skeletal muscle is the muscle fiber. These long, tubular, multinucleated cells are filled with overlapping actin and myosin contractile protein filaments, organized into repeating units termed sarcomeres. Sarcomeres are the basic functional contractile units of muscle fibers and, when viewed using the microscope, are responsible for giving skeletal muscle its well known striated appearance. Muscle fibers are arranged in parallel orientation to each other and are organized into fascicle bundles by connective tissue. This connective tissue forms endomysium surrounding each muscle fiber, perimysium delineating fascicles and epimysium enveloping the entire muscle. This connective tissue merges at the tapered ends of muscles to form tendinous or aponeurotic insertions attaching to bone. The forces generated by the contracting sarcomeres are transmitted by the fibers to the insertions via the internal connective tissue architecture of the muscle (MacIntosh *et al*. 2006; Standring 2008).

Muscle development of the trunk and limbs begins in the paired, segmental somites on either side of the neural tube of embryos (Figure 1). A complex cascade of interactions between multiple transcription factors, including Pax3, Pax7 and the

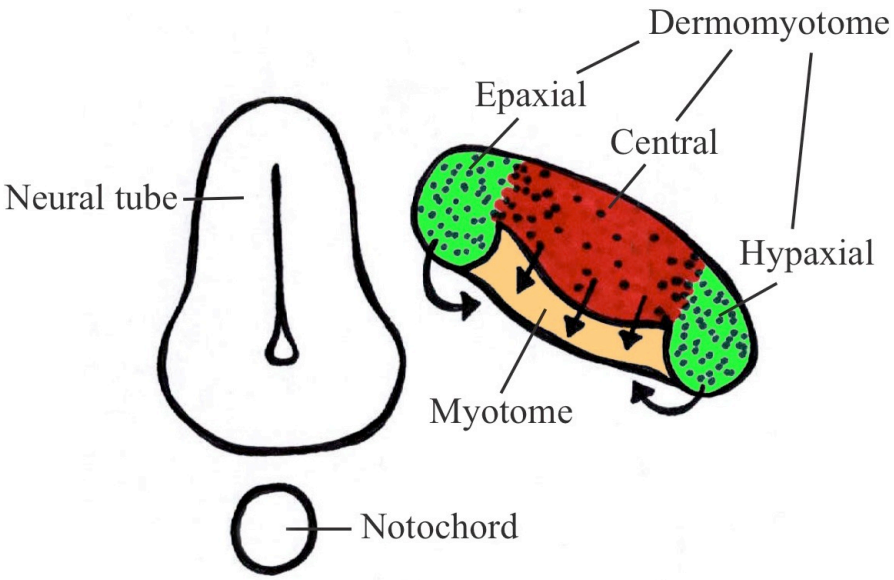

Figure 1 Dermomyotome (DM) and myotome of a mouse thoracic embryonic somite at approximately E9-10. Somites are paired, segmental structures of paraxial mesoderm on either side of the neural tube and notochord. Pax3 (green) is concentrated in epaxial and hypaxial DM, while Pax7 (red) is concentrated in central DM. Myogenic precursor cells migrate from the DM edges into the myotome (arrows). Modified from Buckingham *et al.* 2003, Buckingham *et al.* 2006, and Buckingham and Relaix 2007.

myogenic regulatory factors (MRFs; MyoD, Myf5, myogenin and Mrf4), control the stages of myoblast cell differentiation (Ludolph and Konieczny 1995; Buckingham *et al.* 2006). New findings via genetic labeling suggest that Pax3+/Pax7- cells are precursors to all Pax7 expressing cells (Hutcheson *et al*. 2009). MyoD is drastically reduced in Pax3 homozygous mutant mice (Tajbakhsh *et al.* 1997), and ectopic Pax3 expression induces MyoD and Myf5 expression in chicks (Maroto *et al.* 1997), indicating that Pax3 functions upstream of MyoD and Myf5. The dermomyotome portion of maturing somites is the site of initial expression of Pax3, Pax7, Myf5 and Mrf4. Early cell migration from the dermomyotome populates limb buds and sequesters muscle precursors to the myotome of somites where further myogenic factors such as MyoD and myogenin are expressed, and actin and myosin transcripts begin to appear (Tajbakhsh and Buckingham 2000; Buckingham 2006). MRFs have been generally designated as either "determination factors" (Myf5 and MyoD) or "differentiation factors" (myogenin and Mrf4) based on mutation analyses. In the absence of both Myf5 and MyoD, myoblast precursors are absent and no muscle fibers form. Myogenin homozygous knockout, however, leads to an absence of muscle fibers in the presence of myoblast precursors (Tajbakhsh and Buckingham 2000). Late myogenesis is marked by fusion of myoblast cells into multinucleated myotubes, which grow into muscle fibers. Muscle fibers accumulate in parallel orientation and grow to produce the final product seen in mature organisms (Ludolph and Konieczny 1995).

The Pax gene family encodes nine different paired-box transcription factors crucial for tissue differentiation in early animal development. Pax proteins contain a paired box DNA binding domain, and can have an octapeptide motif and/or part or all of

a homeobox DNA binding domain. Based on the presence or absence of these features, the Pax proteins are divided into 4 subfamilies: Pax3/7; Pax4/6; Pax2/5/8; Pax1/9. Pax3 and Pax7 protein, for example, contain a paired domain, octapeptide and homeodomain with the 1st helix (HD1) and the helix-turn-helix (HD2/3) motif, whereas Pax1 and Pax9 protein contain only a paired domain and octapeptide. Pax proteins are essential for normal development of a vast number of structures (Table 1). Some key examples include Pax6 for eye development, Pax5 for B-lymphocyte production and Pax3/7 for muscle differentiation and maintenance (Chi and Epstein 2002; Buckingham and Relaix 2007; Lang *et al.* 2007).

Pax3 regulates the embryonic development of numerous cell types. The highly pluripotent neural crest cells rely on Pax3 for development and its absence can lead to pigmentation abnormalities, enteric ganglia defects, hearing loss and cardiac defects (Chi and Epstein 2002; Lang *et al.* 2007). Pax3 functions most notably in muscle progenitor cells to regulate their initiation into the myogenic program. Pax3 is initially expressed in pre-somitic paraxial mesoderm before becoming characteristic of established somites. Pax3 is then restricted to the epaxial and hypaxial extremities of the dermomyotome division of somites (Figure 1; Buckingham and Relaix 2007; Galli *et al.* 2008). Pax3 functions upstream of MyoD and Myf5 (Maroto *et al.* 1997; Tajbakhsh *et al.* 1997) and Pax3 expression is down-regulated prior to full-scale expression of MRFs (Williams *et al.* 2000). Pax3 is essential for limb myoblast precursors to delaminate from the somites and migrate to the limb buds (Tajbakhsh *et al.* 1997; Buckingham *et al*. 2003). Pax3 activates the c-Met receptor-encoding gene, which is essential for cell migration (Bladt *et al.* 1995; Epstein *et al.* 1996).

Table 1: Pax gene expression profile and associated human diseases[a]

Pax genes	Embryonic Expression	Associated Human Diseases
Pax1	Skeleton, thymus, 3rd and 4th pharyngeal pouches	Klippel-Feil Syndrome, Jarcho-Levin Syndrome (vertebral malformations)
Pax2	Kidney, CNS, ear	Hyperproliferative dysplastic kidney, renal hyperplasia, bladder and renal cancer, Coloboma Syndrome
Pax3	Somites/skeletal muscle, neural crest, CNS, craniofacial tissue	Waardenburg Syndrome Types I and III, melanoma, rhabdomyosarcoma
Pax4	Pancreas, gut	Diabetes
Pax5	B-lymphocytes, CNS	Lymphomas
Pax6	Pancreas, gut, CNS, nose, eye	Aniridia, GI tumors, cataracts/Peter's Anomaly
Pax7	Somites/skeletal muscle, neural crest, CNS, craniofacial tissue	Melanoma, neuroblastoma, rhabdomyosarcoma
Pax8	Kidney, thyroid, CNS	Congenital hypothyroidism, thyroid carcinomas/adenomas
Pax9	Skeleton, teeth, thymus, craniofacial tissue	Jarcho-Levin Syndrome, oligodentia

[a] Adapted from Chi and Epstein 2002, Buckingham and Relaix 2007 and Lang *et al.* 2007

Pax3 is anti-apoptotic through transcriptional regulation of the anti-apoptotic protein, BCL-XL (Margue *et al.* 2000). Pax3/Pax7 double heterozygous mutant mice have a major loss of skeletal muscle, with only small amounts of muscle developing from early Myf5/Mfr4-expressing myotomal cells, resulting in death at mid-gestation (Relaix *et al.* 2005; Buckingham and Relaix 2007). Pax3 homozygous mutant mice cease development past post-conception day 13 with the absence of limb muscles and increased cell death (Goulding *et al.* 1994; Tremblay *et al.* 1998; Lang *et al.* 2007). Since embryonic Pax3 knockout is lethal and Pax3 expression in muscle is generally down-regulated before birth (Kassar-Duchossoy *et al.* 2005; Horst *et al*. 2006), previous studies on Pax3 have been largely restricted to embryos (Keller *et al*. 2004; Kassar-Duchossoy *et al.* 2005; Relaix *et al.* 2005; Horst *et al.* 2006; Otto *et al*. 2006; Galli *et al*. 2008).

Satellite cells (SCs) are mononuclear myogenic stem cells resting on the surface of multinucleated muscle fibers (Figure 2). First identified by electron microscopy (Mauro 1961), SCs are currently identified by numerous molecular markers, such as Pax7, myocyte nuclear factor, c-Met and M-cadherin (Hawke and Garry 2001). During myogenesis, a subpopulation of Pax3/Pax7-expressing myogenic precursor cells, originally from the dermomyotome, migrate to the surface of developing muscle fibers to become SCs. SCs of the limb muscles are thought to originate from hypaxial dermomyotome (Schienda *et al.* 2006), while SCs of the trunk are derived from central dermomyotome (Gros *et al.* 2005). Inserted between the muscle fiber basal lamina and plasmalemma, SCs are positioned for regulating post-natal muscle growth, regeneration

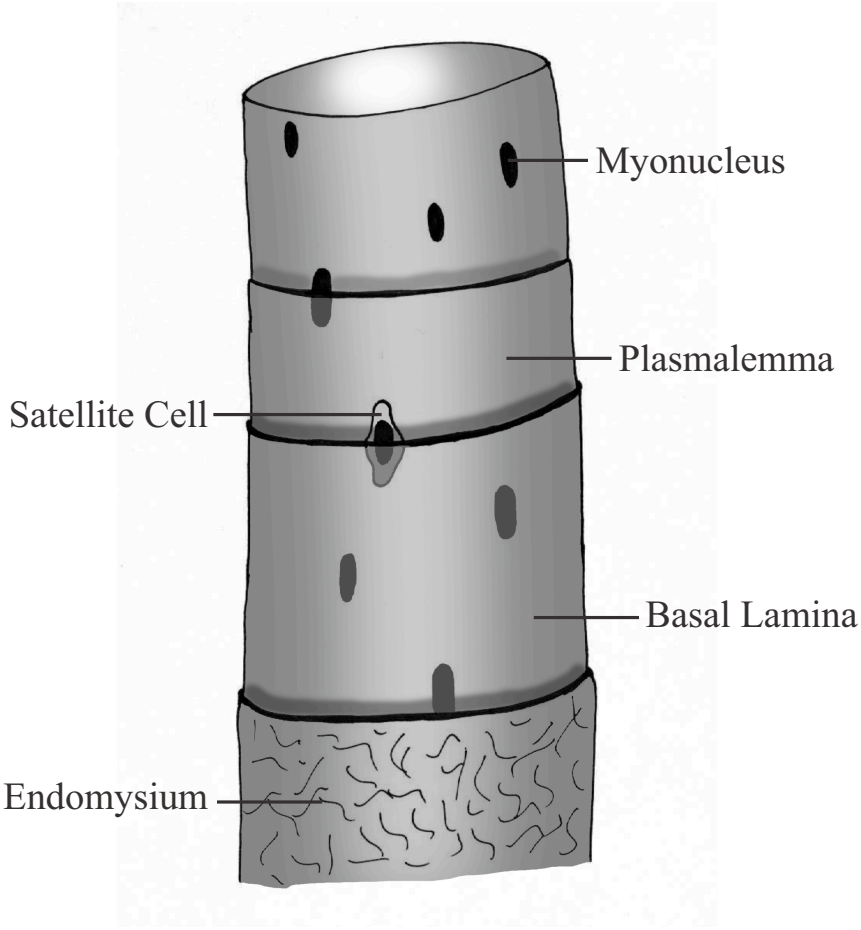

Figure 2 Satellite cell (SC) and myonuclei (MN) within a skeletal muscle fiber. MN are located beneath the plasmalemma within the cytoplasm of muscle fibers. SCs are positioned on the surface of muscle fibers, between the plasmalemma and basal lamina. Endomysium ensheathes each muscle fiber. Modified from Allouh 2007.

and repair (Anderson 2006). Following muscle fiber damage, SCs are triggered to move from a state of quiescence into an activated state, characterized by cell swelling, organelle expansion, and decreased chromatin density, as the cell cycle is initiated. This activation is mediated by the release of nitric oxide from underlying muscle fibers, which leads to the mobilization of hepatocyte growth factor from within damaged fibers to its c-Met receptor on the surfaces of SCs. A cascade of signaling events, potentially including a combination of the mitogen-activated protein kinase pathway, the phosphatidyl inositol 3 kinase pathway, and the adenylate cyclase pathway, regulate subsequent SC proliferation and differentiation to either form new myonuclei (MN) or replenish the existing SC population (Anderson 2000; Wozniak *et al.* 2005; Anderson 2006). Activated SCs migrate to sites of damage and either fuse with existing muscle fibers to become new MN (hypertrophy) or align and fuse together to produce new muscle fibers (hyperplasia; Hawke and Garry 2001). In adult muscle, Pax7 is responsible for SC maintenance through its anti-apoptotic function (Relaix *et al*. 2006). Pax7 homozygous knockout mice die shortly after birth due to SC depletion and subsequent loss of regenerative potential (Seale *et al*. 2000; Lang *et al.* 2007). In normal muscle, decreasing Pax7 expression and increasing MyoD and Mrf5, leads to progression of the myogenic program and subsequent myogenin expression within the new MN. However, by maintaining high levels of Pax7, SCs remain undifferentiated and their population is maintained through self-renewal (Zammit *et al.* 2004; Shinin *et al*. 2006). SC frequency is highest in young muscle, slow contracting fibers, muscle spindles and the tapered ends of fibers, indicating a greater need for fiber growth, regeneration and repair in these regions (Allouh *et al*. 2008; Kirkpatrick *et al.* 2008). SC frequency and concentration

decreases with aging in mature muscle, suggesting a reduced capacity for growth, regeneration and repair during maturation (Kirkpatrick *et al.* 2008). A subset of SCs in a minority of muscles maintain Pax3 expression in mature muscle (Montarras *et al.* 2005; Relaix *et al.* 2006). The function or differential advantage of Pax3 expression in these SCs is currently unknown (Buckingham 2006; Relaix *et al.* 2006; Kuang and Rudnicki 2008).

Muscle spindles are small mechanoreceptors situated within skeletal muscles (Figure 3). Spindles are found in all classes of terrestrial vertebrates and located throughout the body in muscles supplied by either spinal or cranial nerves (Maier 1992). Muscle spindles relay information via their sensory nerves to the central nervous system about the static and dynamic stretch of the muscle in which they are located (Barker *et al.* 1974; MacIntosh *et al*. 2006). This information allows the brain to deduce the relative position of each muscle and the overall arrangement of the body in space (Matthews 1981; Proske 2006). Muscle spindles also receive motor neuron input to allow for contraction of the spindle (Taylor *et al.* 2000). Each spindle consists of tiny intrafusal muscle fibers enclosed within a fusiform-shaped connective tissue capsule that separates the spindle from the much larger extrafusal muscle fibers that make up the bulk of the muscle (De Anda and Rebollo 1967; Maier 1992). Intrafusal fibers of avian and mammalian muscle spindles are classified differently based on the structure of their central regions. Mammalian spindles are categorized as either "nuclear bag" or "nuclear chain" fibers based on a large congregation of nuclei in the central region of "bag" fibers compared to a single line of nuclei in "chain" fibers (Matthews 1964). Intrafusal fibers of birds do not differ as significantly with respect to equatorial nucleation, as there are no

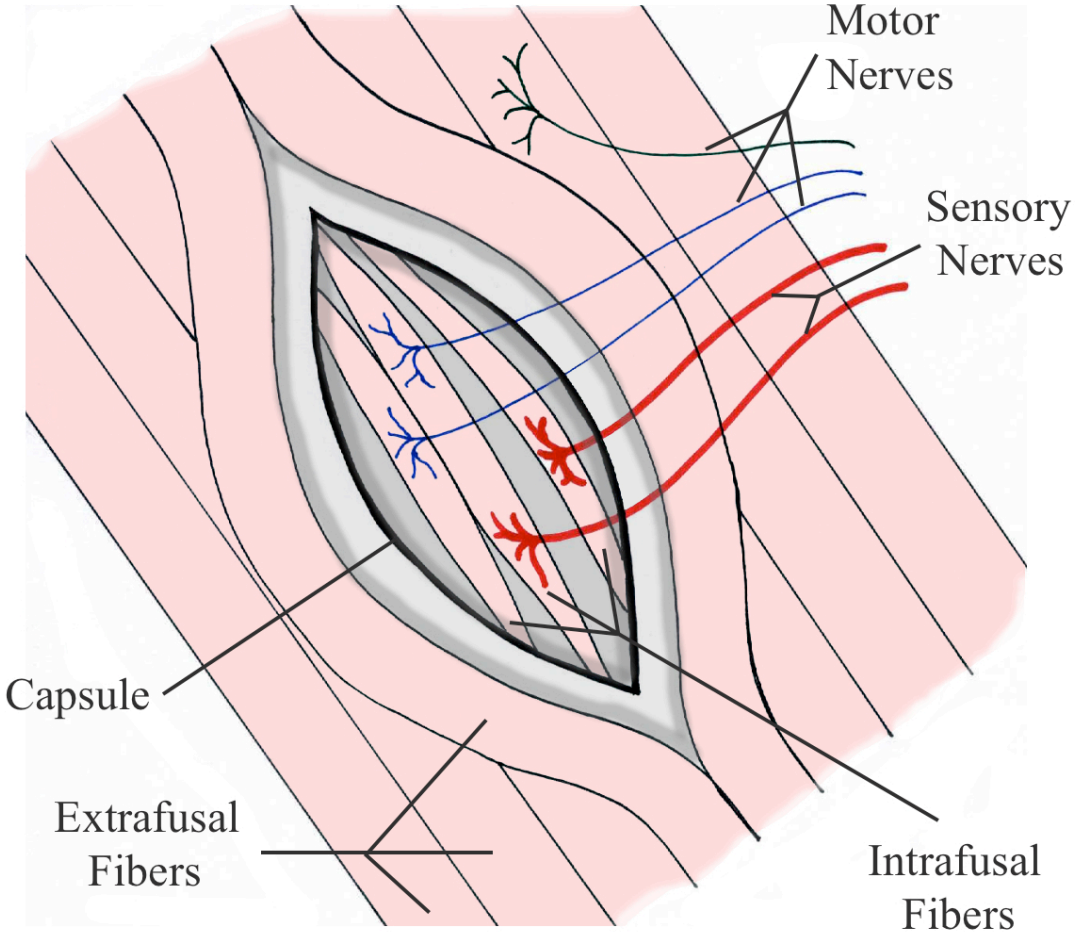

Figure 3 Muscle spindle within avian skeletal muscle. Muscle spindles are composed of several intrafusal fibers enclosed within a connective tissue capsule that is penetrated by sensory and motor nerves. Spindles are orientated in parallel with surrounding extrafusal fibers that compose the bulk of skeletal muscles. Adapted from Maier 1992 and Standring 2008.

nuclear bag fibers. Avian intrafusal fibers are generally divided into "slow" and "fast" groups based on their myosin heavy chain content, myosin ATPase reactivity and overall fiber size (Maier 1992). Intrafusal fibers of muscle spindles maintain characteristics of immature muscle. Expression of developmental myosin heavy chain isoforms (Walro and Kucer 1999), expression of Myf5 (Zammit *et al.* 2004), arrested growth (Kozeka and Ontell 1981), and high SC frequency (Kirkpatrick *et al.* 2008) are all indicators of intrafusal fiber immaturity, which are discussed further in Chapter 3.

Muscle hypertrophy refers to an increase in diameter and/or length in pre-existing muscle fibers, rather than an increase in the number of fibers (hyperplasia), through activation of the insulin-like growth factor 1 signaling pathway responsible for protein synthesis (Glass 2005; Sandri 2008). SC activation can contribute to muscle hypertrophy by providing additional MN to enhance protein synthesis (Hawke and Garry 2001; O'Connor and Pavlath 2007; Ishido *et al.* 2009). Muscle hypertrophy can be experimentally induced via resistance training, electrical stimulation, compensatory overload or stretch (Lowe and Alway 2002). Depending on the hypothesis in question, one model may prove advantageous over others. Synergist tenotomy or ablation has been proved as a proficient compensatory overload model for inducing hypertrophy (Gutmann *et al*. 1970; Gollnick *et al*. 1981; Baldwin *et al.* 1982; Roy *et al.* 1982; Ishido *et al.* 2004). However, it has been suggested that any weight increase seen in the initial stages of this model may be due to inflammation and edema caused by the surgery rather than muscle growth (Armstrong *et al.* 1979; Alway *et al*. 2005). Also, the severed tendon can occasionally reattach itself and undercut further hypertrophy (Lowe and Alway 2002). Thus, caution must be taken when interpreting weight increases in the first 5 days after

surgery (Lowe and Alway 2002). However, the major advantage of synergist tenotomy or ablation is the pronounced and rapid SC activation that occurs as part of the hypertrophic response (Lowe and Alway 2002; Alway *et al.* 2005; Zammit *et al*. 2006). Compensatory overload via synergist tenotomy or ablation is an ideal model for studying SC activation.

The anterior (ALD) and posterior (PLD) latissimus dorsi, formally termed the latissimus dorsi pars cranialis and latissimus dorsi pars caudalis, respectively, are superficial muscles that span the dorsal surface of the shoulder joint in birds and act synergistically to retract and elevate the humerus (Figure 4; Raikow 1985; Vanden Berge and Zweers 1993). The ALD is made up almost exclusively of slow muscle fibers, whereas the PLD consists of mainly fast fibers (Ginsborg 1960). In general, slow fibers reach their peak tension more slowly, are primarily oxidative with high aerobic capacity, while fast fibers reach their peak tension rapidly, are more glycolytic with high anaerobic capacity (George and Berger 1966; Peter *et al*. 1972; Bandman and Rosser 2000). Consequently, the ALD contraction is manifested slowly and maintained for longer periods of time, compared to the PLD which contracts in short sporadic bursts of strength (Bandman and Rosser 2000). The ALD and PLD have long been utilized as experimental models in studies of stretch-induced hypertrophy (Alway 1993; Antonio and Gonyea 1993; Antonio and Gonyea 1994; Carson *et al.* 1995), tenotomy or ablation (Gutmann *et al.* 1970; Jirmanova and Zelena 1970; Gollnick *et al.* 1981; Hikida and Wang 1981), regeneration (Camoretti-Mercado *et al.* 1993), denervation (Jirmanova and Zelena 1970; Gao and Kennedy 1992; Lefeuvre *et al.* 1996), myosin heavy chain content (Gauthier and Orfanos 1993; Rushbrook *et al.* 1997), growth factor effects (Gardahaut *et al.* 1992;

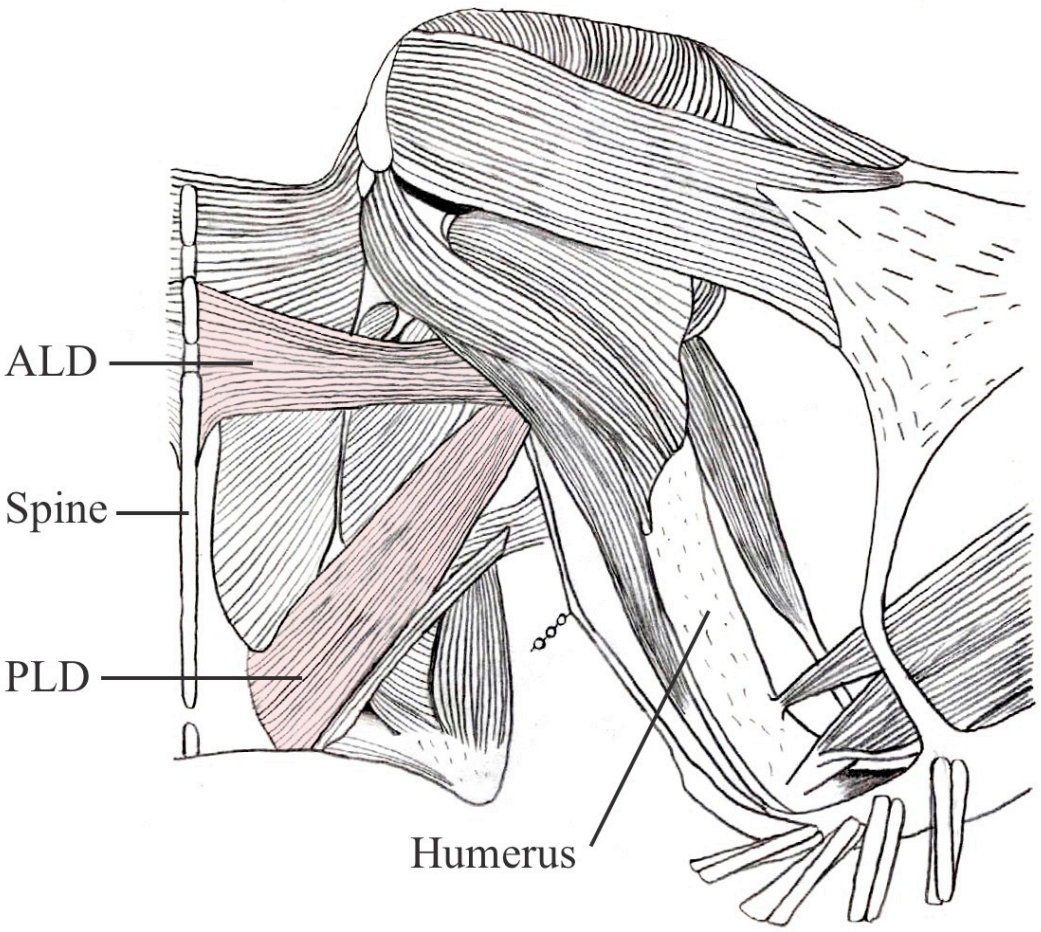

Figure 4 Dorsal view of the right side of the avian thorax and proximal wing, showing the anterior (ALD) and posterior (PLD) latissimus dorsi muscles. The ALD originates on a variable number of cervical and thoracic vertebrae and inserts on the humerus. The PLD originates on thoracic vertebrae and inserts adjacent to the ALD. They act synergistically to adduct the humerus. Adapted from Hudson and Lanzillotti 1955, George and Berger 1966 and Kovacs and Meyers 2000.

Mitchell *et al.* 1999), SCs and MN (Winchester and Gonyea 1992; McCormick and Schultz 1994; Kirkpatrick *et al.* 2008) and muscular dystrophy (Tidyman *et al.* 1997). The synergistic relationship between the ALD and PLD in adducting the avian humerus provides an ideal experimental model for inducing compensatory hypertrophy following synergist tenotomy.

The role of Pax3 in skeletal muscle is only partially understood. While serving distinct functions during embryonic myogenesis, Pax3 is differentially down-regulated in SCs of mature muscle where its expression and functional significance is largely unknown. Intrafusal fibers of muscle spindles are relatively immature compared to the extrafusal fibers of the surrounding muscle. As Pax3 is expressed in muscle progenitors during the early stages of muscle differentiation, this study tests the hypothesis that Pax3 protein maintains localized expression within SCs of muscle spindles. Furthermore, as SCs are induced to proliferate and contribute new MN to overloaded skeletal muscle, this study tests the hypothesis that the proportion of SCs expressing Pax3 protein will increase during conditions of muscle overload. The expression of Pax3 in SCs of muscle spindles is examined during post-hatch development of the chicken ALD. The synergistic relationship of the ALD and PLD is utilized to study Pax3 expression during compensatory PLD overload, and subsequent muscle hypertrophy, following tenotomy of the ALD. Analyzing the presence of Pax3 through post-hatch development and under conditions of SC activation helps to elucidate the expression and function of Pax3 in mature muscle.

Chapter 2:

Specific Aims

Pax3 is essential for myogenesis in developing embryos. However, the function of Pax3 in mature muscle is poorly understood. Limited studies have focused on the post-natal and post-hatch expression of Pax3 and many questions remain unanswered. This thesis examines two fundamental aspects of Pax3 in mature muscle.

1) In Chapter 3, the location and frequency of Pax3 protein expression is determined during ALD post-hatch development. This study tests the hypotheses that Pax3 is expressed at a greater frequency in intrafusal fibers of muscle spindles than in the surrounding extrafusal fibers, and Pax3 expression decreases with age. The percentage of SC and MN expressing Pax3 is calculated in both intrafusal and extrafusal fiber profiles at each age studied.

2) In Chapter 4, the response of Pax3 protein expression under conditions of muscle hypertrophy is examined. This study tests the hypothesis that Pax3 expression is increased with SC activation in response to functional muscle overload. The percentage of SCs and MN expressing Pax3 is calculated in both intrafusal and extrafusal fiber profiles within overloaded and control muscle.

Chapter 3:

Pax3 Expression in Satellite Cells of Post-Hatch Muscle Spindles

3.1 Abstract

Paired box transcription factor three (Pax3) is essential for activation of myogenic regulatory factors in embryos, and is normally expressed in satellite cell (SC) precursors, along with its homologue Pax7. While Pax7 is expressed in all SCs through to maturity, Pax3 is generally repressed in late embryos and appears after birth only in SC subpopulations within select muscles. Intrafusal fibers within muscle spindles retain features characteristic of immaturity, unlike the more numerous adjacent extrafusal fibers. This study tests the hypothesis that Pax3 protein maintains localized expression within SCs of muscle spindles. Immunohistochemical techniques are used to identify SCs by their Pax7 expression, and analyze the proportion of SCs and myonuclei (MN) expressing Pax3 in fiber profiles of anterior latissimus dorsi (ALD) muscle from chickens aged 9, 30, 62 and 145 days post-hatch. Although Pax3 declines with aging, a significantly greater proportion of SCs express Pax3 within intrafusal than extrafusal fiber profiles at each age studied. Also, small numbers of MN express Pax3. Our data suggests that after birth Pax3 may be a component of SC differentiation in muscle. Muscle spindles may provide a novel model for future study of Pax3 and other regulatory genes in mature muscle.

3.2 Introduction

Satellite cells (SCs) are myogenic stem cells located on the surface of skeletal muscle fibers, between plasmalemma and basal lamina (Mauro 1961; Anderson 2006). SCs can be mobilized during muscle growth, maintenance or repair to replicate and differentiate into new MN (Charge and Rudnicki 2004; Collins *et al*. 2005; Zammit *et al*. 2006). Within developing chick embryos, SCs are thought to originate from two cell populations. SCs of the trunk are derived from proliferating central dermomyotome cells (Gros *et al.* 2005), while SCs of the limbs come from hypaxial dermomyotome (Schienda *et al.* 2006). Both populations of SC precursor cells express paired box transcription factors three (Pax3) and seven (Pax7) proteins (Buckingham and Relaix 2007; Galli *et al*. 2008). Pax3 is essential for the activation of myogenic regulatory factors (MRFs; MyoD, Myf5, myogenin, and Mrf4) within proliferating cell populations in embryonic dermomyotome (Relaix *et al.* 2005; Buckingham and Relaix 2007). In mature muscle, SCs are commonly labeled with an antibody against the Pax7 protein (Zammit *et al.* 2006; Day *et al*. 2007), which is expressed by all quiescent and proliferating SCs but not by MN (Seale *et al*. 2000; Halevy *et al*. 2004; Shefer *et al.* 2006). Pax3 protein expression, however, is repressed after embryonic day 13.5 in most mouse trunk and limb muscles of the mouse (Horst *et al.* 2006). Pax3 is only expressed in a varying proportion of SCs within a minority of muscles, such as the diaphragm and gracilis, in post-natal mice (Montarras *et al.* 2005; Relaix *et al.* 2006).

Muscle spindles are minute mechanoreceptors embedded within skeletal muscles (Kokkorogiannis 2004; MacIntosh *et al.* 2006). They relay static and dynamic stretch information about each skeletal muscle to the central nervous system (Barker *et al*. 1974;

MacIntosh *et al.* 2006). Muscle spindles are composed of one to several tiny intrafusal muscle fibers enclosed within a fusiform-shaped connective tissue capsule (De Anda and Rebollo 1967; Maier 1992). This capsule separates the spindle from the much larger extrafusal muscle fibers that make up the bulk of the muscle (Ovalle *et al*. 1999). Intrafusal fibers are believed to persist in a comparatively immature state. Unlike extrafusal fibers, intrafusal fibers maintain developmental myosin heavy chain isoform expression (slow developmental, embryonic, and/or neonatal) characteristic of early myotubes with the potential to become either intrafusal or extrafusal fibers (Walro and Kucera 1999; Liu *et al.* 2002). Intrafusal fibers also maintain expression of Myf5, which is present during the differentiation of skeletal muscle precursors but is down-regulated in mature extrafusal fibers (Zammit *et al*. 2004). In addition, while extrafusal fibers continue to show robust growth until maturity, intrafusal fiber growth is arrested shortly after birth and fibers remain comparatively small (Kozeka and Ontell 1981). Intrafusal fibers maintain greater concentrations of SCs than their surrounding extrafusal fibers (Kirkpatrick *et al*. 2008). This is also indicative of intrafusal fiber immaturity, as SC numbers have been inversely correlated with fiber diameter (Allouh *et al*. 2008) and are greater in younger, smaller diameter fibers within extrafusal fiber populations (Campion 1984; Shefer *et al*. 2006).

This study elucidates the presence and frequency of Pax3 protein expression during post-hatch muscle development. Based upon the rationale that intrafusal fibers are comparatively immature and that Pax3 is normally expressed in SCs of the earlier stages of muscle differentiation, the hypothesis tested is that Pax3 protein maintains localized expression within SCs of muscle spindles. The model studied is anterior latissimus dorsi

(ALD) muscle of the chicken, in which intrafusal fibers have relatively high numbers of SCs (Kirkpatrick *et al.* 2008). Immunohistochemical techniques are used to identify SCs and label Pax3 protein in ALD of several different post-hatch ages. Large proportions of the SCs, and a few MN, were found to express Pax3.

3.3 Materials & Methods

3.3.1 Experimental Model

White Leghorn chickens (*Gallus gallus*; Hy-Line W-36, Clark Hy-Line, Brandon, Canada) were hatched and raised under identical conditions at the University of Saskatchewan, Department of Animal and Poultry Science. Birds were raised in a floor pen on a 23 hour light, one hour dark cycle at an initial temperature of 35°C. Temperature was decreased 3.5°C per week until a final temperature of 21°C was reached when the birds were five weeks post-hatch. Birds were watered and fed *ad libitum* with commercial chick starter until 42 days post-hatch, when they were then fed with a commercial chick grower (Federated Cooperatives Ltd., Saskatoon, Canada). Following the Canadian Council on Animal Care Guidelines, and with the approval of the University of Saskatchewan Committee on Animal Care and Supply, five birds were killed by either cervical dislocation or inhalation of carbon dioxide at 9, 30, 62 and 145 days post-hatch.

3.3.2 Tissue Preparation and Sectioning

The ALD was excised bilaterally from each 9-, 30-, and 62-day bird and from the left side of each 145-day bird. Muscles were weighed, coated with Tissue-Tek OCT Compound (Sakura Finetek; Torrance, CA), and immediately frozen in isopentane cooled by liquid nitrogen (Sewry and Dubowitz 2001). Muscle samples approximately 0.5-1.0 cm x 2-4 cm x thickness of muscle, were removed such that the long axis of each sample was parallel to the direction of the muscle fibers. Right and left ALD muscles were grouped together for analyses of the 9-, 30-, and 62-day birds, and the left ALD muscle

of each 145-day bird was analyzed. Samples were stored at -80°C. Serial cross-sections were cut at 12 micrometer thickness at -20°C using a cryostat. Three serial sections were placed on each ProbeOn Plus charged microscope slide (Fisher Scientific; Nepean, Canada) and sequential slides numbered and stored at -20°C.

3.3.3 Immunohistochemistry

Immunohistochemical techniques were used to analyze cryosections from several locations along the length of each muscle. This ensured that a sufficient number of spindles would be located. Several consecutive slides were labeled at each location along the muscle, permitting comparison and tracking of intrafusal fibers from one section to the next. In analyzing extrafusal fibers, only one location along the muscle was evaluated so that fibers would not be sampled more than once along their lengths.

Primary antibodies used were anti-myosin, anti-laminin, anti-Pax7 and anti-Pax3 (Table 2). Anti-myosin (NA4; gift from Dr. E. Bandman, University of California, Davis, CA; now available at Developmental Studies Hybridoma Bank/DSHB; Iowa City, IA), a mouse monoclonal developed against chicken myosin, was used to detect all myosins of avian skeletal muscle fibers (Moore *et al.* 1992). Anti-laminin (L9393; Sigma Chemical, St. Louis, MO), a rabbit polyclonal raised against the glycoprotein laminin of mice, was used to label basal laminae of skeletal muscle fibers (Vater *et al.* 1994). Anti-Pax7 (DSHB), an IgG_1 isotype mouse monoclonal developed against chicken Pax7 protein, was used to detect SCs (Kawakami *et al.* 1997). Anti-Pax3 (DSHB), an IgG_{2a} isotype mouse monoclonal raised against quail Pax3 protein, was used to detect the Pax3 protein within nuclei (Venters *et al.* 2004). According to information

Table 2 Primary and secondary antibodies and corresponding structure labeled

Primary Antibody	Secondary Antibody	Structure Labeled
Mouse NA4	Green Mouse IgG	Avian Myosin Heavy Chains
Rabbit Anti-laminin	Red Rabbit IgG	Laminin in Basal Laminae
Mouse Anti-Pax3	Green Mouse IgG_{2a}	Pax3 Protein
Mouse Anti-Pax7	Red Mouse IgG_1	Pax7 Protein in SCs
Rabbit Anti-laminin	Blue Rabbit IgG	Laminin in Basal Laminae

supplied by the vendors, the specificity of each primary antibody used included the proper chicken antigen. Appropriate controls, including primary antibodies without secondary antibodies and *vice versa*, were included in each experiment.

The blocking solution consisted of 1% bovine serum albumin (BSA) and 5 mM ethylenediaminetetraacetic acid (EDTA) in phosphate-buffered saline (PBS; 0.02 M sodium phosphate buffer, 0.15 M sodium chloride, pH 7.2), and was applied to each slide for 15-20 minutes at room temperature. The block was then drained from each slide and a primary antibody cocktail was applied overnight at 4°C. The primary antibody cocktail consisted of either (A) 1:400 anti-laminin and 1:5000 anti-myosin diluted in blocking solution, or (B) 1:400 anti-laminin, 1:30 anti-Pax7 and 1:30 anti-Pax3 diluted in blocking solution. Primary antibody cocktails (A) and (B) were alternated with each serial slide. The slides were transferred to Coplin jars and rinsed three times for five minutes each with PBS.

The secondary antibody cocktail added to those slides which received the first primary cocktail (A) consisted of Alexa Fluor 546 goat anti-rabbit IgG (A11010; Invitrogen, Carlsbad, CA) which labels the rabbit anti-laminin red, and Alexa Fluor 488 goat anti-mouse IgG (A11001; Invitrogen) which labels the mouse anti-myosin green. The secondary antibody cocktail applied to slides receiving the other primary cocktail (B)

included Alexa Fluor 350 goat anti-rabbit IgG (A21068; Invitrogen) which labels the rabbit anti-laminin blue, Alexa Fluor 568 goat anti-mouse IgG_1 (A21124; Invitrogen) which labels the mouse anti-Pax7 red, and Alexa Fluor 488 goat anti-mouse IgG_{2a} (A21131; Invitrogen) which labels the mouse anti-Pax3 green. Secondary antibodies in each cocktail were diluted 1:200 in PBS. The appropriate secondary antibody cocktail was applied to each serial slide at room temperature for 30 minutes in the dark. Secondary antibody cocktails were drained and slides were rinsed three times for five minutes each with PBS. Hoechst 33258 (bisbenzimide; Sigma Chemical) was applied to each slide for five minutes at 1:1,500,000 in PBS to label DNA within nuclei blue under epifluorescence. The blue of the bisbenzimide was a lighter hue than the blue of the goat anti-rabbit IgG labeled anti-laminin, so they were easily distinguishable. Slides were drained and rinsed twice for five minutes each with PBS. Finally, 4% formaldehyde in PBS was applied to each slide for three minutes, followed by draining and rinsing twice for five minutes each with PBS. Slides were mounted in Geltol (Thermo Scientific; Pittsburgh, PA) or Aqua-Mount (Lerner Laboratories; Pittsburgh, PA), and stored at 4°C in the dark.

3.3.4 Imaging and Analysis

Results were visualized with a Zeiss Axioskop 20 microscope (Carl Zeiss; Oberkochen, Germany) equipped for epifluorescence, attached to a Sony Cyber-Shot DSC-V3 digital still camera (Sony; Tokyo, Japan). Muscle spindles were located and photographed from sections on serial slides, such that the total number of intrafusal fibers analyzed for each muscle ranged from 30 to 85. Epifluorescent images (red, green and/or

blue), each viewed through a different wavelength filter, were taken of each muscle spindle on adjacent serial slides. Images were transferred to an iMac computer (Apple Computers; Cupertino, CA) and superimposed using Adobe Photoshop (Adobe Systems; San Jose, CA) such that final images consisted of (A) myosin in green and basal laminae in red, and (B) basal laminae in deep blue, all nuclei in light blue, SCs (Pax7) in red, and Pax3 in green.

These images were used to count the number of SCs and MN within each muscle fiber cross-sectional profile, and the proportion of SCs and MN expressing Pax3. In this thesis we use the term "profile" as defined by Coggeshall 1992: "… a slice of a particle (fiber) that appears in a histological section" (Rosser *et al.* 2000). Each fiber boundary was demarcated by its basal lamina. SCs were identified as light blue nuclei expressing red Pax7. Pax3-expressing SCs were noted as light blue nuclei co-expressing red Pax7 and green Pax3. Pax3-expressing MN were recognized as light blue nuclei expressing only green Pax3. All intrafusal fiber profiles examined and 200 adjacent extrafusal fiber profiles from each muscle studied were analyzed in this way. The ellipse minor axis of these same fiber profiles was measured using Scion Image 1.63 (developed by the U.S. National Institutes of Health and available on the internet by anonymous FTP from Zippy.nimh.nih.gov). Ellipse minor axis of Scion Image is identical to lesser fiber diameter (Rosser *et al.* 2000), which is defined as the maximum aspect across the lesser aspect of a fiber. Lesser fiber diameter is routinely used to overcome distortion that may result if a muscle fiber is cut obliquely rather than transversely (Dubowitz and Sewry 2007).

The average number of satellite cell nuclei (SCN) and MN per fiber profile were used to calculate the frequency of SCs in both intrafusal and extrafusal fibers of each muscle studied using the formula SCN frequency = (#SCN/(#SCN+#MN)) x 100% (Schmalbruch and Hellhammer 1977). The proportion of SCs or MN containing Pax3 in both intrafusal and extrafusal fiber profiles of each muscle studied was calculated using the formulae Pax3 positive SCN frequency = (#Pax3 positive SCN/#all SCN) x 100% or Pax3 positive MN frequency = (#Pax3 positive MN/#all MN) x 100%.

3.3.5 Statistics

ALD muscles from five animals at 9-, 30-, 62-, and 145-days post-hatch were studied. Data is presented as means and standard errors. The muscle weight, ellipse minor axis, SC frequency, percentage of Pax3 positive SCs, and percentage of Pax3 positive MN were analyzed at each age. An arcsine transformation was applied to percentage data prior to statistical analysis (Zar 1999; van Emden 2008). Homogeneity of variance was tested via Levene's test, and group means were subsequently evaluated using a one-way analysis of variance (ANOVA) test at 5% level of significance ($p \leq 0.05$). Bonferroni's pairwise comparison between group means was used for *post hoc* analysis when variances were equal, and Tamhane's pairwise comparison when variances were unequal. Statistical test were performed using SPSS 16.0 for Windows (SPSS; Chicago, IL).

3.4 Results

3.4.1 Identifying Structures

Laminin is a major component of the basement membrane in a variety of cell types, including endothelium, nerve and muscle (Tzu and Marinkovich 2008). Muscle fibers were located based on their myosin heavy chain content and laminin-rich basement membrane (Figures 5A,E and 6A,E). To distinguish intrafusal from extrafusal fibers, the thickened, laminin-rich connective tissue capsule of muscle spindles was identified surrounding intrafusal fibers (Figures 5 and 6). SCs in both intrafusal and extrafusal fiber profiles were identified by their Pax7 content and standard position beneath the basal lamina, whereas MN, also located beneath the basal lamina, were recognized by their lack of Pax7 expression (Figures 5C,G and 6C,G). Pax3 protein was localized primarily in a subpopulation of SC nuclei within intrafusal fiber profiles (Figures 5D,H and 6D,H). Pax3 was expressed less frequently in SC nuclei of extrafusal fiber profiles, and rarely within MN of intrafusal or extrafusal fiber profiles (not shown in figures). Nuclei located outside the basal lamina of muscle fiber profiles did not express Pax3.

3.4.2 Anterior Latissimus Dorsi Muscle Weight

Wet weight of ALD muscle increased over 20-fold from 9 to 145 days post-hatch (Figure 7A). Mean ALD weight was 0.019 ± 0.001g (ranging from 0.008 to 0.030g) at 9 days, 0.068 ± 0.004g (from 0.057 to 0.082g) at 30 days, 0.235 ± 0.012g (from 0.192 to 0.268g) at 62 days and 0.400 ± 0.036g (from 0.352 to 0.544g) at 145 days. Muscle weight was significantly different between all ages; 9 vs. 30 days ($p<0.001$), 9 vs. 62

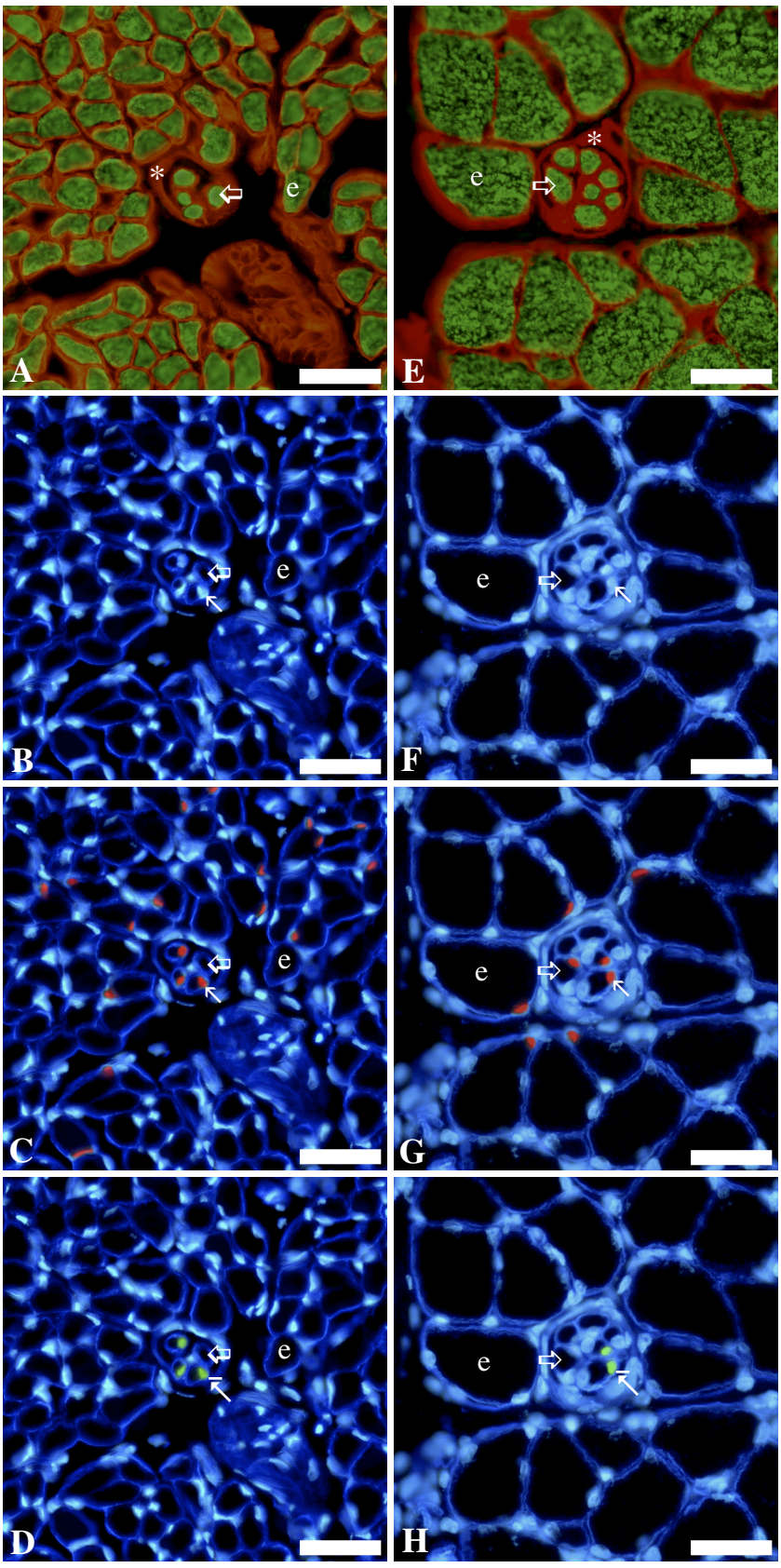
A
E
B
F
C
G
D
H
e
*

Figure 5 Immunohistochemical labeling of serial cross-sections of anterior latissimus dorsi (ALD) muscle: 9 days (A-D), and 30 days (E-H) post-hatch. In each series, the first image (A or E) is from a serial section adjacent to the cross-section from which the subsequent three images (B-D or F-H) are taken. In the first image (A or E), laminin is red and myosin green. In subsequent images, laminin is deep blue and nuclei light blue (B-D or F-H), Pax7 red (C or G) and Pax3 green (D or H). Several intrafusal fibers clustered within a spindle capsule are near the center of each image, and are smaller in diameter than the larger extrafusal fibers that are always situated outside of the capsule. Open/large arrows, intrafusal fibers; small arrows, satellite cells; small arrows with line, satellite cell expressing Pax3; asterisk, capsule of muscle spindle; e, extrafusal fiber. The same representative intrafusal fibers, extrafusal fibers and satellite cell nuclei are labeled in each image throughout each series (A-D, E-H). Each scale bar = 30 microns.

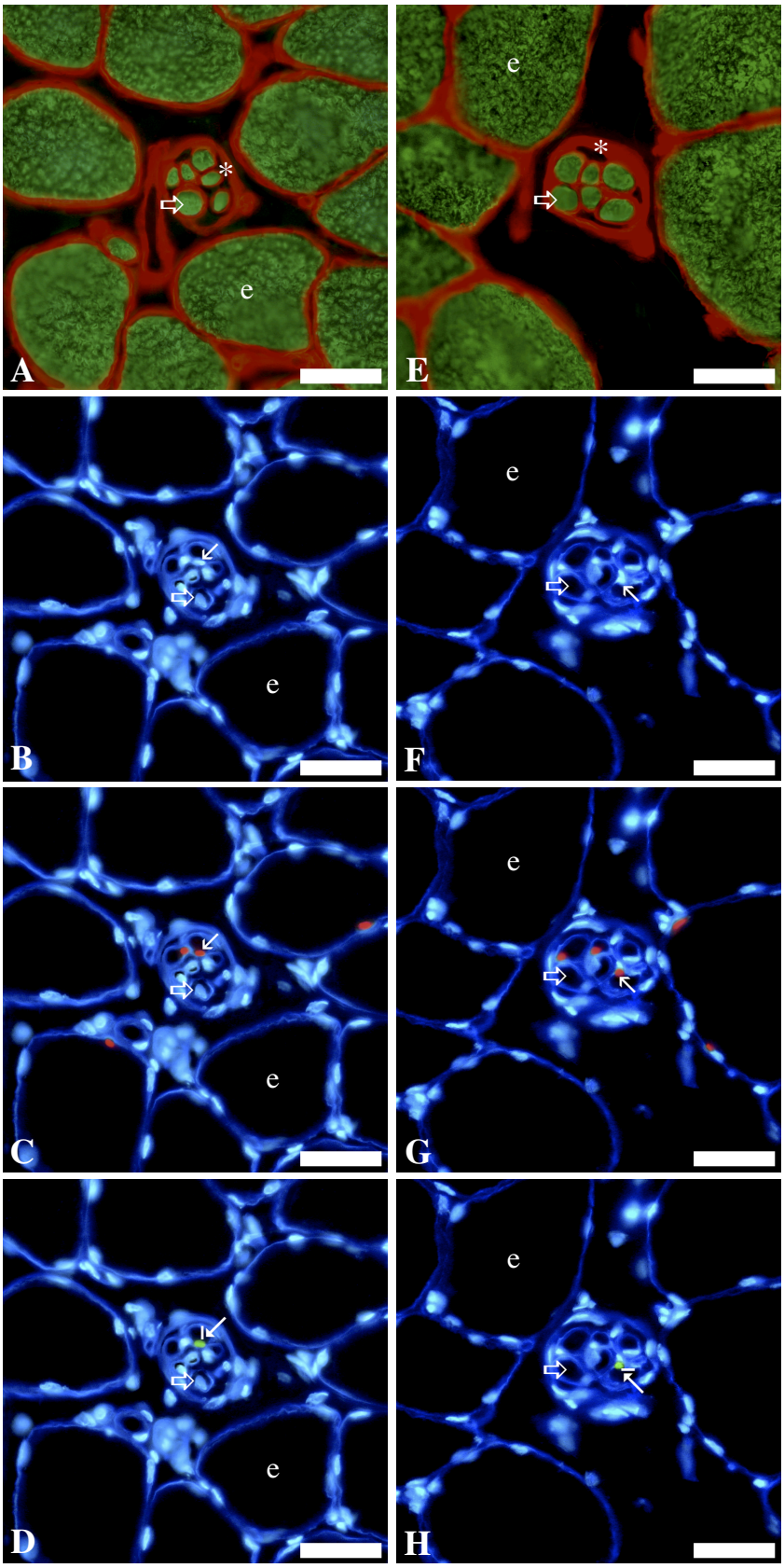
A
e
*
E
e
*
B
e
F
e
C
e
G
e
D
e
H
e

Figure 6 Immunohistochemical labeling of serial cross-sections of anterior latissimus dorsi (ALD) muscle: 62 days (A-D), and 145 days (E-H) post-hatch. In each series, the first image (A or E) is from a serial section adjacent to the cross-section from which the subsequent three images (B-D or F-H) are taken. In the first image (A or E), laminin is red and myosin green. In subsequent images, laminin is deep blue and nuclei light blue (B-D or F-H), Pax7 red (C or G) and Pax3 green (D or H). Labeling scheme is the same as that used in Figure 5. Each scale bar = 30 microns.

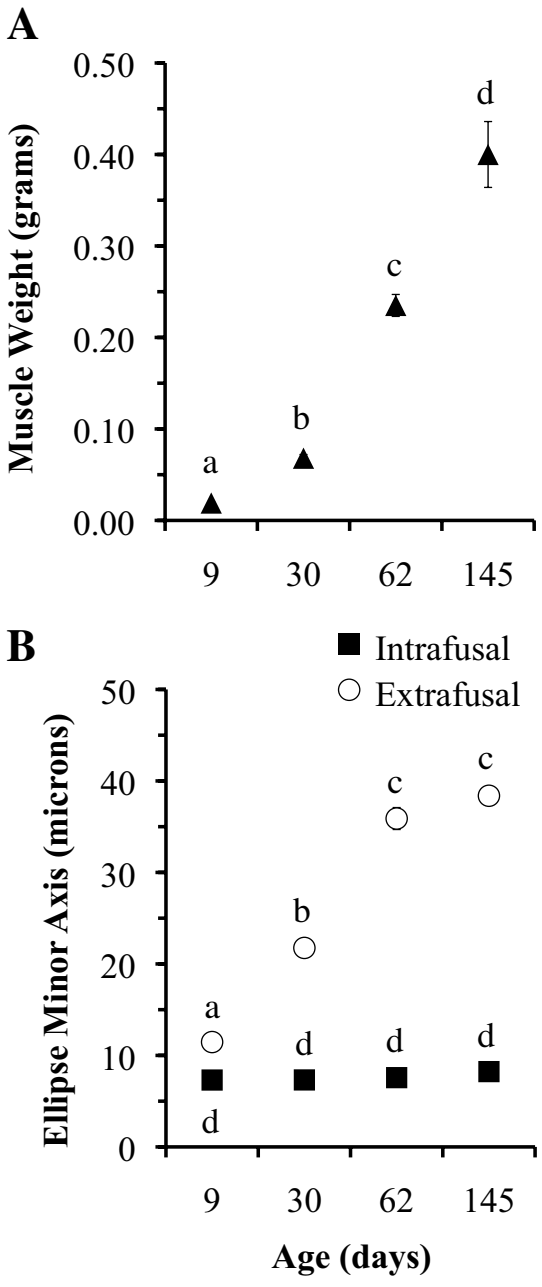
A
Muscle Weight (grams)
0.50
0.40
0.30
0.20
0.10
0.00
a
b
c
d
9
30
62
145
B
Intrafusal
Extrafusal
Ellipse Minor Axis (microns)
50
40
30
20
10
0
a
b
c
c
d
d
d
d
9
30
62
145
Age (days)

Figure 7 Anterior latissimus dorsi (ALD) muscle weight and fiber size data. Muscle weight (A) increases with age. Ellipse minor axis (B) of extrafusal fibers is greater than that of intrafusal fibers. Ellipse minor axis of extrafusal fibers increases with age, but remains constant in intrafusal fibers. Within each graph (A and B), symbols with the same lowercase letter are not significantly different ($p>0.05$) from one another. Symbols with different lowercase letters are significantly different ($p\leq0.05$) from one another. Each value is expressed as mean $\pm$ SE (n=5). Error bars that are not visible are smaller than the symbol used to denote each mean.

days ($p<0.001$), 9 vs. 145 days ($p=0.003$), 30 vs. 62 days ($p<0.001$), 30 vs. 145 days ($p=0.005$), and 62 vs. 145 days ($p=0.05$).

3.4.3 Ellipse Minor Axis

Mean ellipse minor axis of extrafusal fibers increased over 3-fold from 9 to 145 days post-hatch; at 9 days, 11.46 $\pm$ 0.27 micrometers ranging from 10.65 to 12.08 micrometers, at 30 days, 21.75 $\pm$ 0.30 micrometers extending from 20.62 to 22.29 micrometers, at 62 days, 35.89 $\pm$ 1.20 micrometers with a range of 33.95 to 40.53 micrometers, and at 145 days, 38.38 $\pm$ 0.39 micrometers varying from 37.62 to 39.68 micrometers (Figure 7B). Extrafusal fiber ellipse minor axis was significantly different between all ages except 62 and 145 days post hatch ($p=0.960$); 9 vs. 30 days ($p<0.001$), 9 vs. 62 days ($p<0.001$), 9 vs. 145 days ($p<0.001$), 30 vs. 62 days ($p=0.005$) and 30 vs. 145 days ($p<0.001$). Conversely, ellipse minor axis of intrafusal fibers did not change with age (Figure 3B); 9 vs. 30 days ($p=1.000$), 9 vs. 62 days ($p=1.000$), 9 vs. 145 days ($p=0.800$), 30 vs. 62 days ($p=1.000$), 30 vs. 145 days ($p=0.238$), and 62 vs. 145 days ($p=0.933$). The overall mean intrafusal fiber ellipse minor axis for all ages was 7.64 $\pm$ 0.28 micrometers, ranging from a minimum of 6.50 to a maximum of 8.83 micrometers.

3.4.4 Satellite Cell Frequency

Mean frequency of SCs (Figure 8A) was significantly ($p\leq0.001$) higher in intrafusal than extrafusal fiber profiles at each of the four ages studied. Mean SC frequency for all ages was 30.40 $\pm$ 2.32% (ranging from 22.64 to 38.46%) in intrafusal

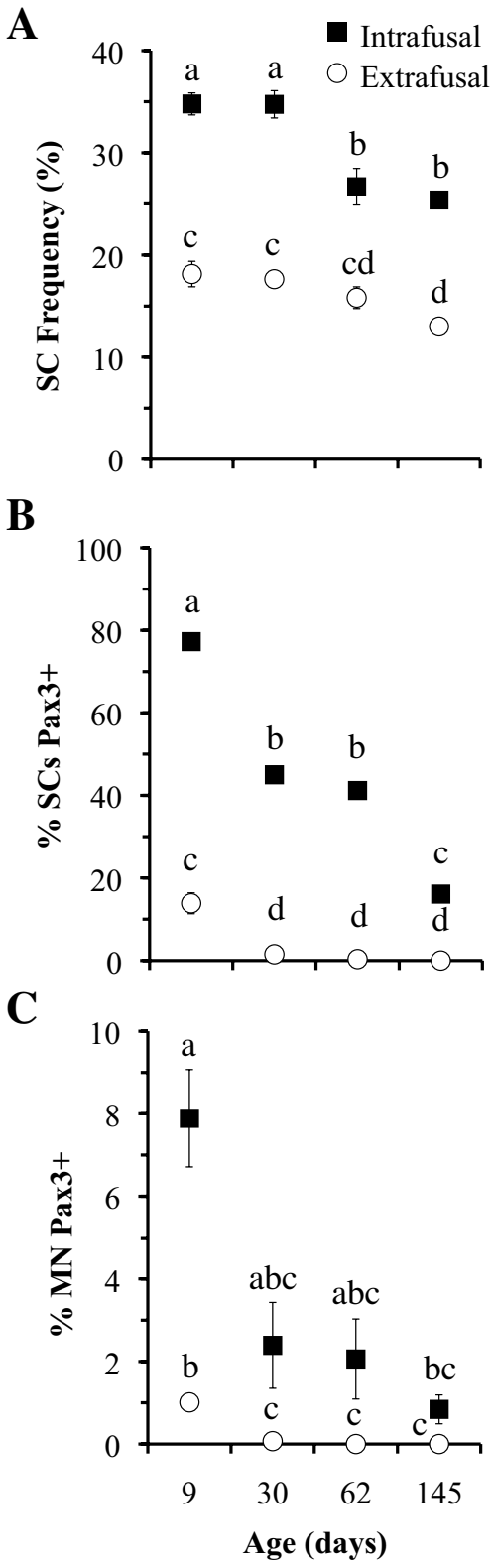
A
Intrafusal
Extrafusal
SC Frequency (%)
40
30
20
10
0
a
a
b
b
c
c
cd
d
B
% SCs Pax3+
100
80
60
40
20
0
a
b
b
c
c
d
d
d
C
% MN Pax3+
10
8
6
4
2
0
a
abc
abc
b
bc
c
c
c
9
30
62
145
Age (days)

Figure 8 Anterior latissimus dorsi (ALD) muscle intrafusal and extrafusal fiber nuclei data. Satellite cell (SC) frequency (A) is greater in intrafusal than extrafusal fiber profiles at each age studied, and, with aging, decreases in both intrafusal and extrafusal fiber profiles. Percentage of SCs expressing Pax3 (B) is also higher in intrafusal than extrafusal fiber profiles at each age studied and also decreases with age. Percentage of myonuclei (MN) expressing Pax3 (C) is initially higher in intrafusal than extrafusal fiber profiles, but decreases with age to be statistically the same in intrafusal and extrafusal fiber profiles. Within each graph (A-C), symbols with the same lowercase letter are not significantly different ($p>0.05$) from one another. Symbols with different lowercase letters are significantly different ($p\leq0.05$) from one another. Each value is expressed as mean $\pm$ SE (n=5). Error bars that are not visible are smaller than the symbol used to denote each mean.

fiber profiles and 16.15 ± 1.26% (varying from 11.89 to 20.68%) in extrafusal fiber profiles. Overall, SC frequency decreased within both intrafusal and extrafusal fiber profiles with age. Within intrafusal fiber profiles, SC frequency decreased significantly from 30 to 62 days post-hatch ($p \leq 0.001$). SC frequency in intrafusal fiber profiles stayed constant from 9 to 30 days ($p=1.000$) and from 62 to 145 days ($p=1.000$) post-hatch. Within extrafusal fiber profiles, SC frequency decreased significantly by 145 days post-hatch; 9 vs. 30 ($p=1.000$), 9 vs. 62 ($p=1.000$), 9 vs. 145 days ($p=0.017$), 30 vs. 62 ($p=1.000$), 30 vs. 145 ($p=0.040$), 62 vs. 145 ($p=1.000$).

3.4.5 Satellite Cells Expressing Pax3

Mean percentage of SCs expressing Pax3 (%SCs Pax3+; Figure 8B) was significantly ($p \leq 0.009$) higher in intrafusal than extrafusal fiber profiles at each age studied, and at all ages except when comparing 9-day extrafusal and 145-day intrafusal fiber profiles ($p=1.000$). Within intrafusal fiber profiles, %SCs Pax3+ was highest at 9 days with a range of 73.91 to 82.35% (mean of 77.26 ± 1.49%), decreasing to 38.10 to 50.00% (average of 45.00 ± 2.00%) at 30 days, 36.36 to 45.00% (mean of 41.18 ± 1.38%) at 62 days, and 12.00 to 19.05% (average of 16.08 ± 1.23%) at 145 days post-hatch. Within intrafusal fiber profiles, mean %SCs Pax3+ was significantly ($p<0.001$) different between all ages, with the exception of 30 and 62 days post-hatch ($p=0.992$). Within extrafusal fiber profiles, mean %SCs Pax3+ at 9 days was 13.85 ± 2.53%, ranging from 9.26 to 21.62%. However, mean %SCs Pax3+ declined to less than 2% by 30 days, and became zero by 145 days post-hatch. The mean %SCs Pax3+ within extrafusal fiber profiles at 9 days post-hatch was significantly ($p \leq 0.013$) different from

that in extrafusal fiber profiles at each of the other ages studied, but did not change from 30 days onward; 30 vs. 62 (p=0.919), 30 vs. 145 (p=0.400), and 62 vs. 145 (p=0.996).

3.4.6 Myonuclei Expressing Pax3

Mean percentage of MN expressing Pax3 (%MN Pax3+; Figure 8C) was highest in the 9-day intrafusal fiber profiles at 7.89 $\pm$ 1.18% with a range of 5.71 to 12.00%, which was significantly (p=0.008) different from the 9-day extrafusal fiber profiles at 1.01 $\pm$ 0.19% which varied from 0.45 to 1.60%. After 9 days, intrafusal fiber profile mean %MN Pax3+ declined to 2.39 $\pm$ 1.04% ranging from 0.00 to 4.88% at 30 days, 2.06 $\pm$ 0.97% varying from 0.00 to 4.55% at 62 days and 0.84 $\pm$ 0.35% ranging from 0.00 to 1.52% at 145 days post-hatch. In extrafusal fiber profiles, mean %MN Pax3+ decreased to 0.07 $\pm$ 0.07% extending from 0.00 to 0.33% at 30 days and became zero for all five animals at both 62 and 145 days post-hatch. No significant difference in mean %MN Pax3+ was found between intrafusal and extrafusal fiber profiles at 30 (p=0.939), 62 (p=0.904) or 145 (p=0.872) days post-hatch. Within intrafusal fiber profiles, except between 9 vs. 145 days (p=0.015), there was no significant difference in %MN Pax3+ between the various ages studied; 9 vs. 30 days (p=0.539), 9 vs. 62 days (p=0.392), 30 vs. 62 days (p=1.000), 30 vs. 145 days (p=1.000), and 62 vs. 145 days (p=1.000). Within extrafusal fiber profiles, %MN Pax3+ at 9 days was significantly different from 30 (p=0.013), 62 (p=0.016), and 145 (p=0.016) days post-hatch. However, in extrafusal fiber profiles, mean %MN Pax3+ was not significantly different (p=1.000) among 30, 62 and 145 days post-hatch.

3.5 Discussion

This study is the first to localize Pax3 expression within SCs of muscle spindles. It is generally held that Pax3 expression is down-regulated before birth (Kassar-Duchossoy *et al.* 2005; Horst *et al*. 2006). Thus, most previous investigations of Pax3 expression in muscle have been largely restricted to embryos (Keller *et al*. 2004; Kassar-Duchossoy *et al.* 2005; Relaix *et al.* 2005; Horst *et al.* 2006; Otto *et al*. 2006; Galli *et al*. 2008). Only subsets of SCs have been found to maintain Pax3 expression within extrafusal fibers of a minority of post-natal muscles (Montarras *et al.* 2005; Relaix *et al.* 2006). Northern blots have been applied to show Pax3 in homogenates of adult guinea pig diaphragm (Jin *et al*. 2007). RT-PCR analysis has revealed greater Pax3 expression in mouse diaphragm than hindlimb muscles (Day *et al*. 2007). Immunocytochemical techniques have been used to identify abundant Pax3-expressing SCs within the diaphragm and gracilis of 3-week post-natal mice (Relaix *et al*. 2006). The proportion of SCs expressing Pax3 in the diaphragm of these mice was reported to be 85%. Percentages of Pax3-expressing SCs in other muscles were not quantified, but said to be lower than that of the diaphragm. SCs in most ventral trunk and about half of the forelimb muscles studied expressed Pax3, while Pax3 expression was scarce in hindlimb muscles. Reasons for the differential expression of Pax3 between muscles of mice are unclear, as it was concluded that Pax3 expression was not related to fiber type, innervation or embryological origin (Relaix *et al.* 2006).

A greater percentage of Pax3-expressing SCs are associated with intrafusal fiber profiles of muscle spindles than with the surrounding extrafusal fiber profiles, regardless of post-hatch age studied and despite a decline in the percentage of Pax3-expressing SCs

with aging. The reason for greater Pax3 in muscle spindles may be concomitant with other factors indicative of muscle spindle immaturity. Developmental myosin heavy chains (Liu *et al*. 2002), Myf5 expression (Zammit *et al.* 2004), greater SC frequency (Kirkpatrick *et al.* 2008) and small diameters (Kozeka and Ontell 1981) are all indicators of immaturity in muscle spindles. The adaptive advantage in intrafusal fibers maintaining a comparatively immature state is unknown. Muscle spindles are constantly monitoring length changes in skeletal muscle, and intrafusal fibers frequently adjusting their own lengths (Dorward 1970; Vallbo 1974; Maier 1992). This may subject intrafusal fibers to a greater degree of wear and damage than experienced by the large majority of extrafusal fibers. Maintaining numerous factors associated with early muscle development, such as Pax3, may aid in intrafusal fiber repair and preservation.

During maturation, Pax3-expressing SCs decline in number, just as overall SC frequency declines. The decrease of SC numbers with maturation has been previously shown in intrafusal and extrafusal fibers (Kirkpatrick *et al*. 2008), and has been related to a weakened capacity for growth, regeneration and repair (Shefer *et al.* 2006; Brack and Rando 2007). However, during maturation there is a disproportionate decrease in the subset of the SC population that expresses Pax3. This suggests that rather than being a developmental vestige, Pax3-expressing SCs in maturing post-hatch muscle may be performing some function that is repressed.

This study also shows Pax3-expressing MN at a greater frequency in intrafusal fiber profiles than in the surrounding mature extrafusal fiber profiles. Pax3 positive MN have been identified previously in mature mouse diaphragm (Montarras *et al*. 2005; Relaix *et al*. 2006). The role of these nuclei in mature muscle remains to be established.

As Pax3 is known to function upstream of the MRFs MyoD and Myf5 (Maroto *et al.* 1997; Tajbakhsh *et al.* 1997; Relaix *et al.* 2006), key proteins in the differentiation of SCs into MN (Zammit *et al*. 2006), Pax3+/Pax7- nuclei may be in transition from SCs to MN. Pax3 is also known to regulate c-Met (Epstein *et al*. 1996; Keller *et al.* 2004), a receptor critical in migration of myogenic progenitors (Birchmeier and Brohmann 2000). Perhaps these MN express Pax3 as part of their fusion from SCs on the surface of muscle fibers to nuclei within fibers. Future experiments that extend labeling to include MyoD, other MRFs, c-Met and additional proteins involved in myogenesis could provide a better understanding of the exact role of Pax3 positive MN.

ALD muscle wet weight was shown to increase during the developmental period studied. This post-hatch growth occurs through increases in diameter and/or length in pre-existing muscle fibers (hypertrophy), rather than an increase in the number of muscle fibers (hyperplasia; Gollnick *et al.* 1981; Gollnick *et al.* 1983; Antonio and Gonyea 1993). This hypertrophy is restricted to extrafusal fibers whose size increases with age (Ono *et al.* 1993; Tamaki and Uchiyama 1995), as intrafusal fibers reach their maximum size and number shortly after birth (Kozeka and Ontell 1981). The results of this study concur, as throughout post-hatch development extrafusal fiber diameter increases dramatically, while intrafusal fiber size remains consistently small.

Muscle spindles provide a novel model for the study of Pax3 expression in mature muscle. Intrafusal fibers are ideal for studying Pax3 expression in SCs, as they maintain higher SC frequencies than the surrounding extrafusal fibers (Kirkpatrick *et al*. 2008). By identifying a unique source of Pax3-expressing SCs in muscle spindles, the potential for studying Pax3 may be broadened to include muscles thought to be devoid of Pax3 in

mature muscle. In addition, determining how Pax3 responds under stress conditions could provide insight into its function in mature muscle. A variety of experimental protocols including hypertrophy (Maynard and Tipton 1971; Maier *et al*. 1972; Botterman and Edgerton 1975; Hutton and Atwater 1992), atrophy (Maier *et al.* 1972; Estavillo *et al*. 1973; Zhu *et al*. 2008), denervation (Schroder 1974; Zelena and Soukup 1993; Walro *et al.* 1997) and neuromuscular block (Taylor *et al.* 1994; Rosales *et al*. 1996) have been used to study intrafusal fibers of muscle spindles. Future studies may employ these or other experimental procedures to explore Pax3 expression in SCs. The muscle spindle model may prove to be a useful tool in future experiments aiming to broaden our understanding of the roles and interrelationships of regulatory genes in mature muscle.

Chapter 4:

Pax3 Expression Increases with Muscle Overload

4.1 Abstract

Pax3 protein is a vital activator of the myogenic program in early development of skeletal muscle. Subsequently, Pax3 is down-regulated and becomes limited to a fraction of satellite cells (SCs) in select mature muscles. Functional overload of skeletal muscle leads to SC activation and muscle hypertrophy. This study tests the hypothesis that experimental muscle overload leads to an increase in Pax3 expression in mature muscle. Functional overload is induced in posterior latissimus dorsi (PLD) muscle via tenotomy of the synergist anterior latissimus dorsi (ALD) in mature animals. Seven days after tenotomy, PLD muscles were removed and analyzed using immunohistochemical methods. Pax3, SCs and myonuclei (MN) were labeled in cross-sections of mature experimental, mature control and young control muscles. Compensatory hypertrophy of the mature PLD leads to percentages of both Pax3+ SCs and Pax3+ MN in intrafusal and extrafusal fiber profiles comparable to those observed in young muscle, and significantly greater than those of mature control. SC activation in response to functional muscle overload results in a disproportionate increase in the percentage of SCs expressing Pax3. Thus, it appears as if Pax3 expression in mature muscle is not a developmental vestige, but expressed in activated SCs.

4.2 Introduction

The Pax gene family is composed of nine transcription factors that function during organogenesis to regulate cellular proliferation, renewal and differentiation (Chi and Epstein 2002; Lang *et al.* 2007). During myogenesis, a complex web of interations between multiple transcription factors, including two Pax proteins and the myogenic regulatory factors (MRFs; MyoD, Myf5, myogenin, and Mrf4), allow multipotent cells to determinate, differentiate and develop into mature muscle (Ludolph and Konieczny 1995; Buckingham *et al.* 2006). Within proliferating cell populations in the dermomyotome of embryos, the activation of MRFs is incumbent upon Pax genes. In Pax3/Pax7 double homozygous mutants, cells do not enter the myogenic program and resultant skeletal muscle defects are associated with death at mid-gestation (Relaix *et al.* 2005). In Pax3 homozygous knockout mice that cease development past post-conception day 13, limb muscles do not form and there is an increase in cell death due to the loss of Pax3's anti-apoptotic role (Goulding *et al*. 1994; Tremblay *et al*. 1998; Lang *et al*. 2007). In Pax7 homozygous knockouts, seven-day-old mice are 50% smaller than controls (Seale *et al*. 2000). However, MRFs are still expressed and skeletal muscle develops normally (Seale *et al*. 2000), likely due to Pax3's ability to compensate for the lack of Pax7 (Lang *et al*. 2007). Pax3 cannot replace Pax7 in SC maintenance, however, as SCs undergo apoptosis and are progressively lost in Pax7 homozygous knockouts (Oustanina *et al.* 2004; Relaix *et al*. 2006; Buckingham 2007).

SCs are myogenic stem cells located on the surface of skeletal muscle fibers, between plasmalemma and basal lamina (Mauro 1961; Anderson 2006). SCs can be

mobilized during muscle growth or repair to replicate and differentiate into new MN (Charge and Rudnicki 2004; Collins *et al*. 2005; Zammit *et al*. 2006). In mature muscle, all SCs express Pax7 but no MN express Pax7 (Halevy *et al*. 2004; Shefer *et al.* 2006; Day *et al*. 2007). Pax3 is co-expressed with Pax7 in SC precursor cells in the embryo (Buckingham and Relaix 2007; Galli *et al*. 2008), but is only present in a varying fraction of SCs in a subset of mature muscles (Relaix *et al*. 2006). In this thesis, previous findings from the study of post-hatch ALD muscle show that, in post-hatch ALD muscle, Pax3 protein maintains greater localized expression within SCs of muscle spindles than in the surrounding extrafusal fiber profiles (see Chapter 3). These results may be related to the relative immaturity of muscle spindles as compared to the surrounding extrafusal fibers. Muscle spindles are known to maintain developmental isoforms of myosin heavy chain (Liu *et al*. 2002), Myf5 expression usually associated with myogenesis (Zammit *et al.* 2004), small diameters (Kozeka and Ontell 1981) and high SC numbers (Kirkpatrick *et al.* 2008). Muscle spindles are very active, constantly monitoring skeletal muscle stretch (Dorward 1970; Vallbo 1974; Maier 1992). Maintaining developmental features associated with high growth and regeneration potential may curb some of the expected intrafusal fiber damage associated with the high activity levels of muscle spindles.

Skeletal muscle hypertrophy is an increase in muscle mass or girth that occurs through the activation of complex signaling pathways responsible for protein synthesis and growth in pre-existing muscle fibers (Glass 2005; Sandri 2008). SCs play an important role in this process through their activation, proliferation and differentiation into additional MN to enhance protein synthesis (Hawke and Garry 2001; O'Connor and Pavalth 2007; Ishido *et al*. 2009). Hypertrophy occurs naturally during development and

with progressive resistance exercise, but can also be induced experimentally via resistance training, electrical stimulation, compensatory overload or stretch (McDonagh and Davies 1984; Timson 1990; Lowe and Alway 2002). Each experimental model has advantages and disadvantages in studying hypertrophy, and each has made important contributions to understanding the mechanisms by which hypertrophy occurs (Alway *et al.* 2005). Tenotomy (severing the tendon) or ablation (complete removal) of synergistic muscles is a commonly employed method of inducing compensatory overload. Eliminating the action of one muscle of a synergistic pair functionally overloads the remaining intact muscle (Lowe and Alway 2002). This method has been used to induce hypertrophy in a variety of animals and muscles (Gutmann *et al.* 1970; Jirmanova and Zelena 1970; Adams *et al*. 1999; Ishido *et al.* 2004; Hyatt *et al.* 2008). A major advantage of synergist tenotomy or ablation is the pronounced and rapid hypertrophic response of the intact muscle, which is ideal for activating SCs (Lowe and Alway 2002; Alway *et al.* 2005; Zammit *et al*. 2006).

This study tests the hypothesis that muscle overload increases the proportion of SCs expressing Pax3 protein in both intrafusal and extrafusal muscle fibers. The rationale is that SCs are activated in response to muscle overload and that Pax3 protein expression is maintained within some SCs of intrafusal and, to a lesser extent, extrafusal fibers of mature muscle. The model used to stimulate SC activation is the synergistic ALD and PLD muscles of the chicken, both of which arise on vertebral spines to insert upon the humerus to adduct the wing (Raikow 1985). Surgically severing the ALD tendon induces rapid hypertrophy of the ipsilateral PLD. Immunohistochemical techniques are used to identify SCs and label Pax3 protein in PLD harvested 7 days after

tenotomy from both the ipsilateral (mature experimental) and contralateral (mature control) sides of 145-day post-hatch birds, as well as un-operated 30-day post-hatch PLD. The number of Pax3-expressing SCs increases in response to muscle overload.

4.3 Materials & Methods

4.3.1 Experimental Model

White Leghorn chickens (*Gallus gallus*; Hy-Line W-36, Clark Hy-Line, Brandon, Canada) were hatched and raised by the Department of Animal and Poultry Science, at the University of Saskatchewan. All chicks were kept on a 23-hour light, one-hour dark cycle at 35°C in a floor pen. Room temperature was decreased 3.5°C per week until 21°C was reached when the birds were aged five weeks post-hatch. Birds were watered and fed *ad libitum* with commercial chick starter until 42 days post-hatch, when they were switched to commercial chick grower (Federated Cooperatives Ltd., Saskatoon, Canada).

Unilateral tenotomy was performed on the right ALD muscle of five 138-day post-hatch birds, to cause mechanical stress on the synergistic PLD muscle. Chickens were anesthetized initially by inhalation of 5% isoflurane (Abbott Laboratories; Saint-Laurent, Canada) and maintained with 1.5-2% isoflurane through surgery. Birds were intubated with 3.5 ET tubes (Smiths Medical; Markham, Canada) and given 0.2 mg/kg meloxicam (Boehringer Ingelheim; Burlington, Canada) intramuscularly in breast muscle. An incision was made on the dorsal thorax adjacent to the spine, and the right ALD was severed at its origin. The left side remained intact for use as a control. Incisions were closed with tissue glue and/or skin staples when necessary. A second dose of 0.1 mg/kg meloxicam was given the day following surgery. Seven days after tenotomy, the five 145-day post-hatch birds were killed by inhalation of carbon dioxide. The seven day time point was chosen to avoid any immediate complications associated with surgery, but include the large SC activation that occurs rapidly after compensatory

overload as the primary objective of this study (Lowe and Alway 2002; Alway *et al.* 2005). An additional five un-operated 30-day post-hatch were killed by cervical dislocation. All protocols for surgery and euthanasia were approved by the University of Saskatchewan Committee on Animal Care and Supply, and followed the Canadian Council on Animal Care Guidelines.

4.3.2 Tissue Preparation and Sectioning

The PLD was excised bilaterally from each 30- and 145-day post-hatch bird. Muscles were weighed, coated with Tissue-Tek OCT Compound (Sakura Finetek; Torrance, CA), frozen in isopentane cooled by liquid nitrogen (Sewry and Dubowitz 2001), and stored at -80°C. The right and left PLD muscles were analyzed separately as experimental and control groups, respectively, for the 145-day tenotomized animals. Serial cross-sections from each muscle studied were cut at 12 micrometer thickness using a cryostat at -20°C. Three serial sections were placed on each ProbeOn Plus charged microscope slide (Fisher Scientific; Nepean, Canada) and consecutive slides numbered and stored at -20°C.

4.3.3 Immunohistochemistry

Blocking solution was first applied to groups of serial slides from several locations along the length of each muscle. The blocking solution consisted of 1% bovine serum albumin (BSA) and 5 mM ethylenediaminetetraacetic acid (EDTA) in phosphate-buffered saline (PBS; 0.02 M sodium phosphate buffer, 0.15 M sodium chloride, pH 7.2). The block was applied to each slide for 15-20 minutes at room

temperature, and then drained from each slide and a primary antibody cocktail was applied to the slides.

The primary antibody cocktail contained either (A) 1:400 anti-laminin and 1:5000 anti-myosin diluted in blocking solution, or (B) 1:400 anti-laminin, 1:30 anti-Pax7 and 1:30 anti-Pax3 diluted in blocking solution. Primary antibody cocktails (A) and (B) were alternated with each serial slide. Anti-myosin (DSHB; Iowa City, IA), a mouse monoclonal developed against chicken myosin, was used to detect all myosins of avian skeletal muscle fibers (Moore *et al.* 1992). Anti-laminin (L9393; Sigma Chemical, St. Louis, MO), a rabbit polyclonal raised against the glycoprotein laminin of mice, was used to label basal lamina of skeletal muscle fibers (Vater *et al*. 1994). Anti-Pax7 (DSHB), an IgG_1 isotype mouse monoclonal developed against chicken Pax7 protein, was used to locate SCs (Kawakami *et al*. 1997). Anti-Pax3 (DSHB), an IgG_{2a} isotype mouse monoclonal against quail Pax3 protein, was used to detect the Pax3 protein within nuclei (Venters *et al.* 2004). Each antibody was obtained commercially and its specificity for the appropriate chicken protein was confirmed by the vendor. Suitable controls, including primary antibodies without secondary antibodies and *vice versa*, were included in each experiment. The primary antibodies were applied overnight at 4°C, then rinsed three times for five minutes each with PBS. Two secondary antibody cocktails were then alternately applied to each serial slide for 30 minutes at room temperature in the dark.

The secondary antibody cocktails consisted of either (A) Alexa Fluor 546 goat anti-rabbit IgG (A11010; Invitrogen, Carlsbad, CA) which labels the rabbit anti-laminin red, and Alexa Fluor 488 goat anti-mouse IgG (A11001; Invitrogen) which labels the mouse anti-myosin green, or (B) Alexa Fluor 350 goat anti-rabbit IgG (A21068;

Invitrogen) which labels the rabbit anti-laminin blue, Alexa Fluor 568 goat anti-mouse IgG_1 (A21124; Invitrogen) which labels the mouse anti-Pax7 red, and Alexa Fluor 488 goat anti-mouse IgG_{2a} (A21131; Invitrogen) which labels the mouse anti-Pax3 green. Each secondary antibody was diluted 1:200 in PBS. Secondary antibody cocktails were drained and slides rinsed three times for five minutes each with PBS.

Hoechst 33258 (bisbenzimide; Sigma Chemical) was applied at a dilution of 1:1,500,000 in PBS to each slide for five minutes to label DNA within nuclei blue, under epifluorescence. As the blue of the bisbenzimide was a lighter hue than that of the goat anti-rabbit IgG labeled anti-laminin, they were readily discerned. Slides were drained and rinsed twice for five minutes each with PBS. Slides were then fixed with 4% formaldehyde in PBS for three minutes, and then drained and rinsed twice for five minutes in PBS. Lastly, slides were mounted in either Geltol (Thermo Scientific; Pittsburgh, PA) or Aqua-Mount (Lerner Laboratories; Pittsburgh, PA), and stored at 4°C in the dark.

4.3.4 Imaging and Analysis

Muscle spindles were located and photographed on serial slides, such that the total number of intrafusal fiber profiles analyzed for each muscle ranged from 30 to 60. Spindles were visualized with a Zeiss Axioskop 20 microscope (Carl Zeiss; Oberkochen, Germany) equipped for epifluorescence, and photographed with an attached Sony Cyber-Shot DSC-V3 digital still camera (Sony; Tokyo, Japan). The red, green and blue epifluorescent images were transferred to an iMac computer (Apple Computers; Cupertino, CA) and superimposed using Adobe Photoshop (Adobe Systems; San Jose,

CA) such that the final images consisted of (A) myosin in green and basal lamina in red, and (B) basal lamina in deep blue, nuclei in light blue, SCs in red, and Pax3 in green.

All intrafusal fiber profiles and 200 adjacent extrafusal fiber profiles from each animal were imaged this way, and subsequently analyzed for number of SCs and MN per fiber cross-sectional profile and the proportion of SCs and MN expressing Pax3. The ellipse minor axis of the same fiber profiles was measured using Scion Image 1.63 (developed by the U.S. National Institutes of Health and available on the internet by anonymous FTP from Zippy.nimh.nih.gov). Ellipse minor axis is the same as lesser fiber diameter (Rosser *et al*. 2000), which is commonly used to correct for distortion resulting from an obliquely rather than transversely cut muscle fiber (Dubowitz and Sewry 2007).

The average number of satellite cell nuclei (SCN) and MN per fiber cross-sectional profile in each animal was used to calculate the frequency of SCs in both intrafusal and extrafusal fiber profiles using the formula SCN frequency = (#SCN/(#SCN+#MN)) x 100% (Schmalbruch and Hellhammer 1977). The average percentage of SCs or MN containing Pax3 in both intrafusal and extrafusal fiber profiles in each animal were calculated using the formulae Pax3 positive SCN frequency = (#Pax3 positive SCN/#all SCN) x 100% or Pax3 positive MN frequency = (#Pax3 positive MN/#all MN) x 100%.

4.3.5 Statistics

PLD muscles from five animals at 30- and 145-days post-hatch were studied. The left (mature control) and right (mature experimental) PLD muscles of the 145-day post-hatch tenotomized birds were analyzed as separate groups. Data is presented as

means and standard errors. The muscle weight, ellipse minor axis, SC frequency, percentage of Pax3 positive SCs, and percentage of Pax3 positive MN were analyzed in each group. An arcsine transformation was applied to percentage data prior to statistical analysis (Zar 1999; van Emden 2008). Differences between mature control and mature experimental group means were evaluated using a Paired-Samples T-Test at 5% significance level. Differences between the 30-day group mean and each of the mature group means were evaluated first for homogeneity of variance via Levene's test, and subsequently evaluated using a one-way analysis of variance (ANOVA) test at 5% level of significance ($p \leq 0.05$). When variances were equal, Bonferroni's pairwise comparison between group means was used for *post hoc* analysis. Tamhane's pairwise comparison was utilized when variances were unequal. The frequency of fibers with small (<20 micrometers), medium (20-60 micrometers) and large (>60 micrometers) ellipse minor axes was compared between mature control and mature experimental groups by Chi-square analysis at 5% level of significance (McClung *et al.* 2005). Statistical test were performed using SPSS 16.0 for Windows (SPSS; Chicago, IL).

4.4 Results

4.4.1 Identifying Structures

Muscle fiber profiles were identified by their green-labeled myosin heavy chain content and red-labeled laminin-rich basement membrane, in cross-sections of PLD muscle (Figure 9A, E and I). Intrafusal fiber profiles were situated within a thickened laminin-rich muscle spindle capsule, and were smaller in diameter than the surrounding extrafusal fibers. Nuclear profiles were identified by viewing adjacent serial cross-sections of PLD muscle under different fluorescent filters (Figure 9B, F and J; Figure 9C, G and K; Figure 9D, H and L). MN and SCs were labeled by bisbenzamide as light blue structures situated within the muscle fiber borders, which were demarcated by dark blue-labeled laminin (Figure 9B, F and J). SCs were those nuclei also labeled red for Pax7 deep to basal laminae (Figure 9C, G and K). MN were identified by their lack of red-labeled Pax7 deep to basal laminae. Pax3-expressing SCs were identified as a subpopulation of green-labeled SCs (Figure 9D, H and L). Less common Pax3-expressing MN were also observed (Figure 9L). Nuclei outside basal laminae did not show labeling for Pax7 or Pax3.

4.4.2 Posterior Latissimus Dorsi Muscle Weight

Wet weight of PLD muscle is greater with experimental overload (mature expt.) than unaltered control contralateral PLD (mature ctrl.) in mature animals (Figure 10A). The absolute difference between mature experimental and mature control muscles ranged from 0.03 to 0.2g. The difference in wet weight with experimental overload as a percent of control ranged from 104% to 121%. Although PLD muscle weight was greater with

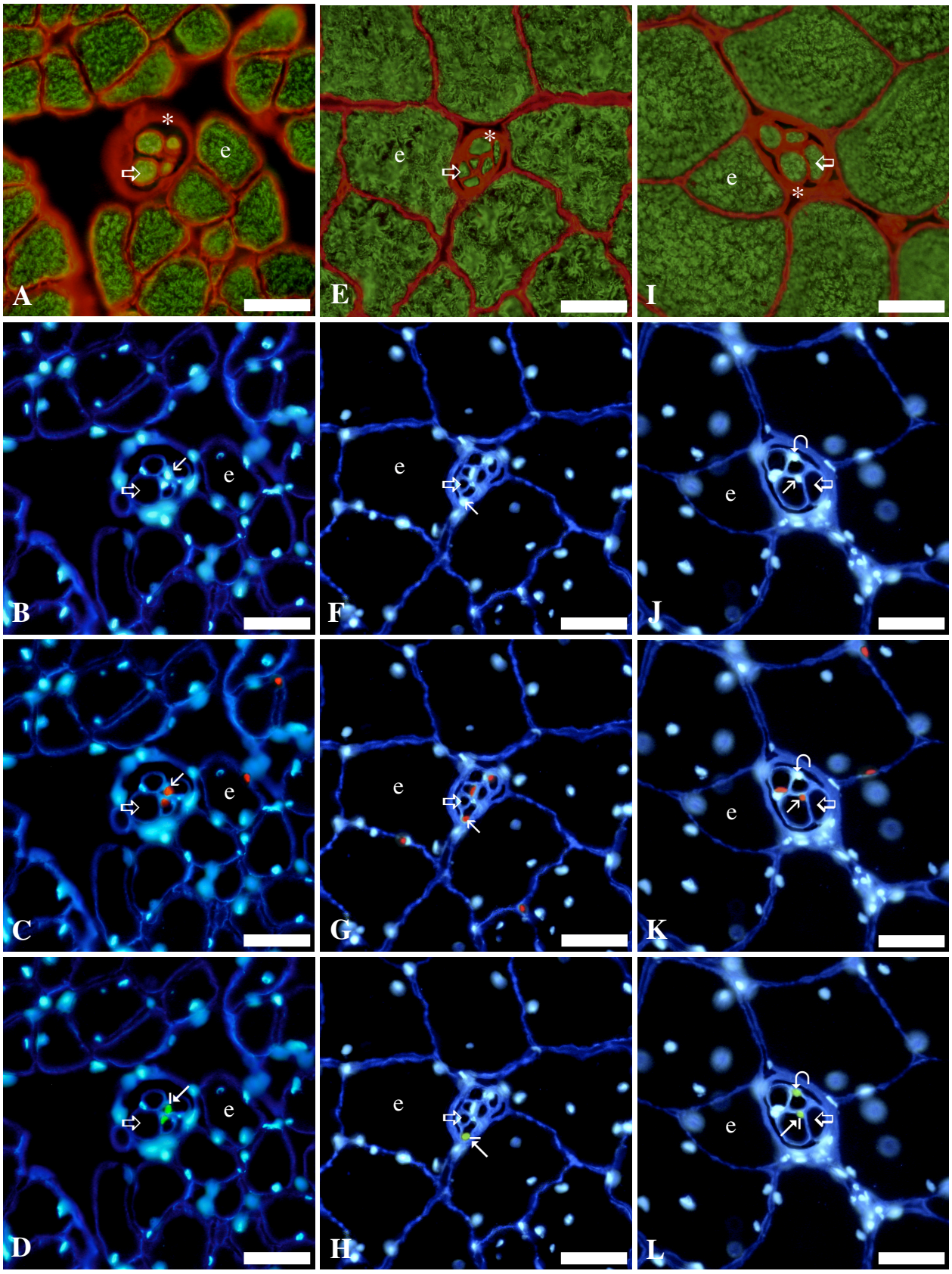
A
E
I
B
F
J
C
G
K
D
H
L
e
*

Figure 9 Immunohistochemical labeling of serial cross-sections of posterior latissimus dorsi (PLD) muscle: 30 day (A-D), mature control (E-H), and mature experimental (I-L) post-hatch. In each series, the first image (A, E or I) is from a serial section adjacent to the cross-section from which the subsequent three images (B-D, F-H or J-L) are taken. In the first image (A, E or I), laminin is red and myosin green. In subsequent images, laminin is deep blue and nuclei light blue (B-D, F-H or J-L), Pax7 red (C, G or K) and Pax3 green (D, H or L). Several intrafusal fibers clustered within a spindle capsule are near the center of each image, and are smaller in diameter than the larger extrafusal fibers situated outside of the capsule. Open/large arrows, intrafusal fibers; small arrows, satellite cells; small arrows with line, satellite cell expressing Pax3; curved arrows, myonucleus expressing Pax3; asterisk, capsule of muscle spindle; e, extrafusal fiber. The same representative intrafusal fibers, extrafusal fibers and nuclei are labeled in each image throughout each series (A-D, E-H or I-L). Each scale bar = 30 microns.

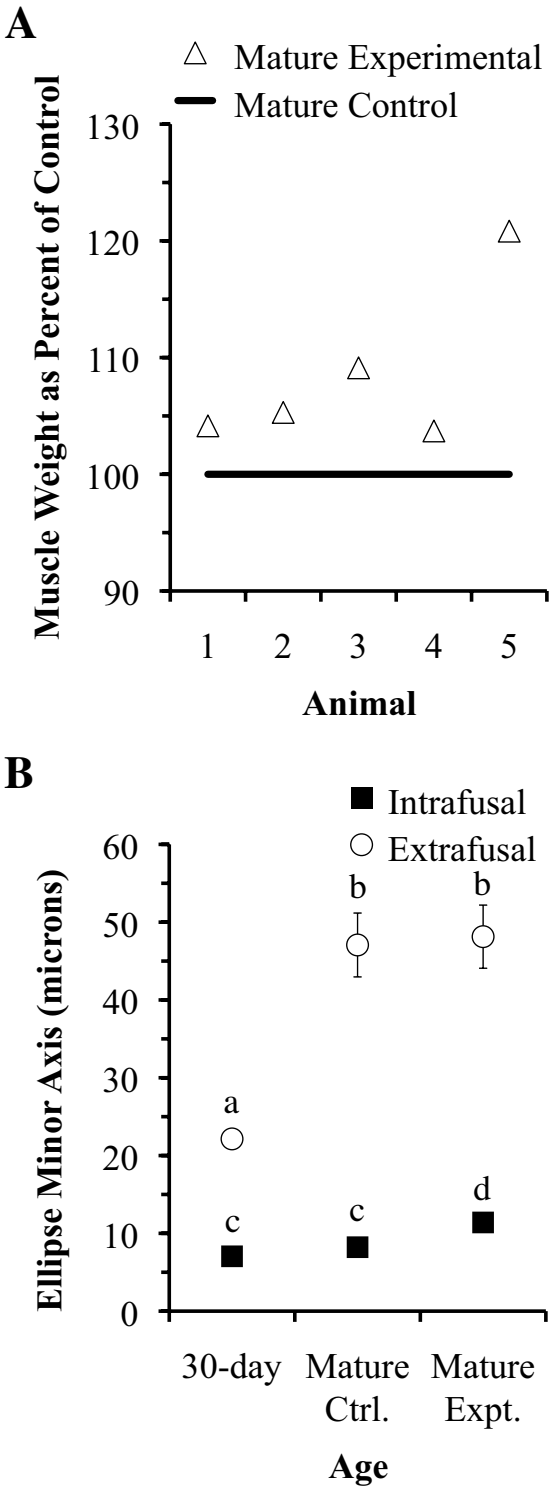
A
Mature Experimental
Mature Control
Muscle Weight as Percent of Control
130
120
110
100
90
1
2
3
4
5
Animal
B
Intrafusal
Extrafusal
Ellipse Minor Axis (microns)
60
50
40
30
20
10
0
a
b
b
c
c
d
30-day
Mature Ctrl.
Mature Expt.
Age

Figure 10 Posterior latissimus dorsi (PLD) muscle weight and fiber size data. Muscle weight (A) is greater with experimental muscle overload (mature expt.) versus control (mature ctrl.). In each group studied, ellipse minor axis (B) of extrafusal fibers is greater than that of intrafusal fibers. Although ellipse minor axis of extrafusal fibers shows an increase in size from 30 to 145 days (mature ctrl.) post-hatch, that of intrafusal fibers remains unchanged with aging. Intrafusal fiber size is, however, increased with muscle overload. In graph B, symbols beneath the same lowercase letter are not significantly different ($p>0.05$) from one another. Symbols beneath different lowercase letters are significantly different ($p\leq0.05$) from one another. Each value is expressed as mean $\pm$ SE (n=5). Error bars that are not visible are smaller than the symbol used to denote each mean.

overload in each animal, the mean muscle weight of all five animals together was not significantly different between mature control and mature experimental groups ($p=0.066$). This was due to variation in muscle weight between animals. PLD wet weight ranged from 0.723 to 1.038g in mature control animals and from 0.753 to 1.160g in experimentally overloaded (mature expt.) animals.

4.4.3 Ellipse Minor Axis

Mean ellipse minor axis (Figure 10B) was greater in extrafusal than intrafusal fibers in 30-day ($p<0.001$), mature control ($p=0.010$), and mature experimental ($p=0.012$) groups. Within intrafusal fibers, mean ellipse minor axis was greater with experimental muscle overload (mature expt.) compared to the mature control ($p=0.008$) or the 30-day ($p=0.001$) group. Ellipse minor axes of the 30-day and mature control groups were statistically the same ($p=0.600$). Intrafusal fiber ellipse minor axis of the 30-day and the mature control animals ranged from 5.92 to 9.02 micrometers, with a mean of 7.05 ± 0.40 micrometers for 30-day animals and 8.22 ± 0.34 micrometers for mature control animals. Intrafusal fiber ellipse minor axis of experimentally overloaded mature animals ranged from 10.63 to 11.88 micrometers, with an average of 10.54 ± 0.89 micrometers. Extrafusal fiber ellipse minor axis was significantly less in the 30-day group, at 22.14 ± 0.60 micrometers (extending from 20.56 to 23.32 micrometers), than either the mature control ($p=0.05$) or mature experimental ($p=0.04$) groups, at 47.07 ± 4.11 micrometers (ranging from 42.38 to 63.47 micrometers) and 48.14 ± 4.06 micrometers (varying from 38.33 to 60.01 micrometers), respectively. However, there was no significant ($p=0.746$) difference in mean ellipse minor axis of extrafusal fibers between the mature

experimental and mature control groups. Nonetheless, the frequency distribution of extrafusal fiber ellipse minor axes was significantly different ($p<0.001$) with experimental overload than in mature control animals. The frequency of extrafusal fibers with both relatively tiny (<20 micrometers) or giant (>60 micrometers) ellipse minor axes was greater with muscle overload (mature expt.) as compared to the mature control group, whose fibers tended to fall closer to the mean fiber size (20-60 micrometers; Figure 11).

4.4.4 Satellite Cell Frequency

Mean SC frequency (Figure 12A) was greater in intrafusal than extrafusal fiber profiles in the 30-day, mature control, and mature experimental groups ($p<0.001$). Intrafusal fiber profile SC frequency ranged from 22.22 to 28.89% (mean of 24.95 $\pm$ 1.15%) in the 30-day group, from 17.54 to 20.69% (average of 19.62 $\pm$ 0.57%) in the mature control group and 21.98 to 25.58% (mean of 24.00 $\pm$ 0.65%) in the mature experimental group. Within intrafusal fiber profiles, SC frequency decreased with age from the 30-day to the mature control groups ($p=0.001$). Experimental overload increased mean SC frequency significantly ($p=0.012$) from mature control values, to levels not different ($p=1.000$) from those of the 30-day animals. Extrafusal fiber profile SC frequency in 30-day and mature control groups was 9.74 $\pm$ 0.06% and 8.57 $\pm$ 0.18%, respectively, and ranged from 7.90 to 9.94%. Extrafusal fiber profile SC frequency in the mature experimental group was 15.32 $\pm$ 1.17%, varying from 12.09 to 19.28%. Within extrafusal fiber profiles, SC frequency decreased with age from the 30-day group to the mature control group ($p<0.001$), but was greater with

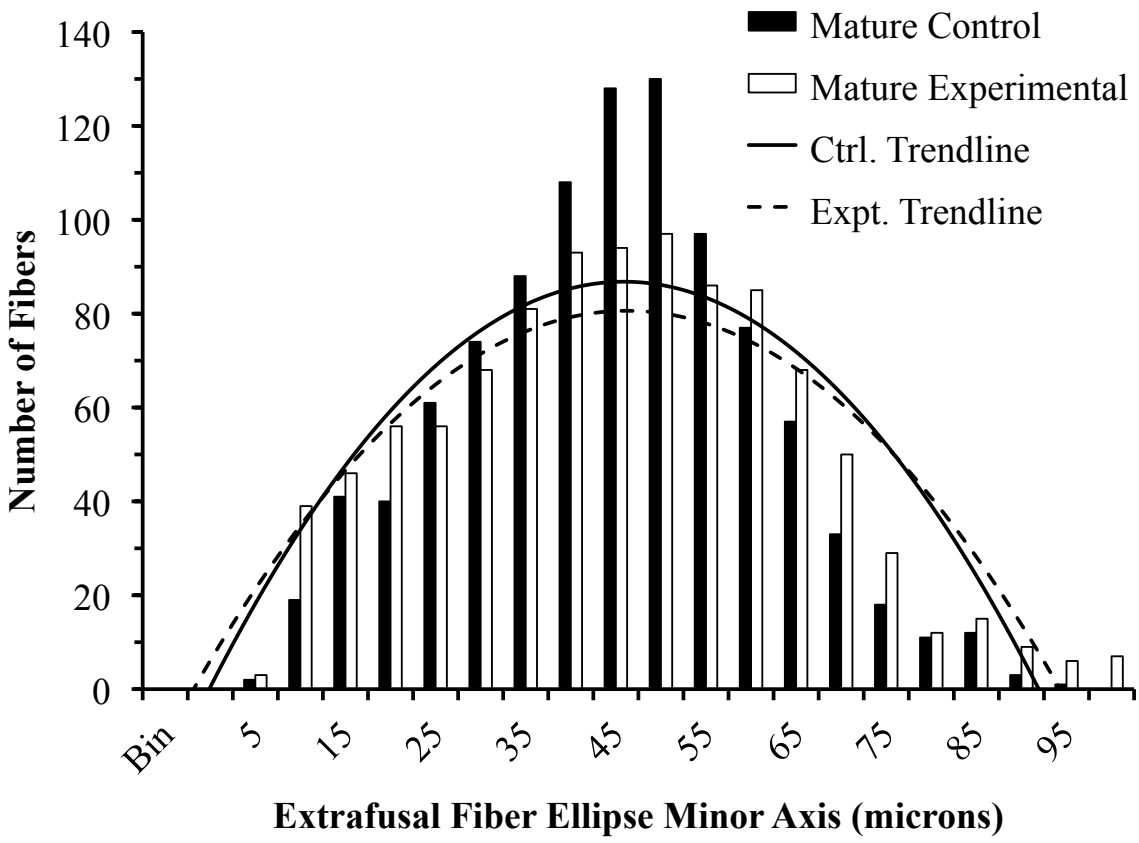

Figure 11 Histogram of ellipse minor axis of extrafusal fibers in posterior latissimus dorsi (PLD) muscle. Experimental (expt.) data is higher in the tails of the curve, while control (ctrl.) data is higher in the center of the curve. This demonstrates that muscle overload (experimental) leads to more smaller and larger diameter fibers. Trendlines are second order polynomials with equations $y = -1.0248x^2 + 22.916x – 41.305$ for control and $y = -0.872x^2 + 19.612x – 29.656$ for experimental. For each group, 200 extrafusal fibers were measured for each animal (n=5). Thus, the graph depicts the ellipse minor axes of 1,000 control fibers and 1,000 experimental fibers.

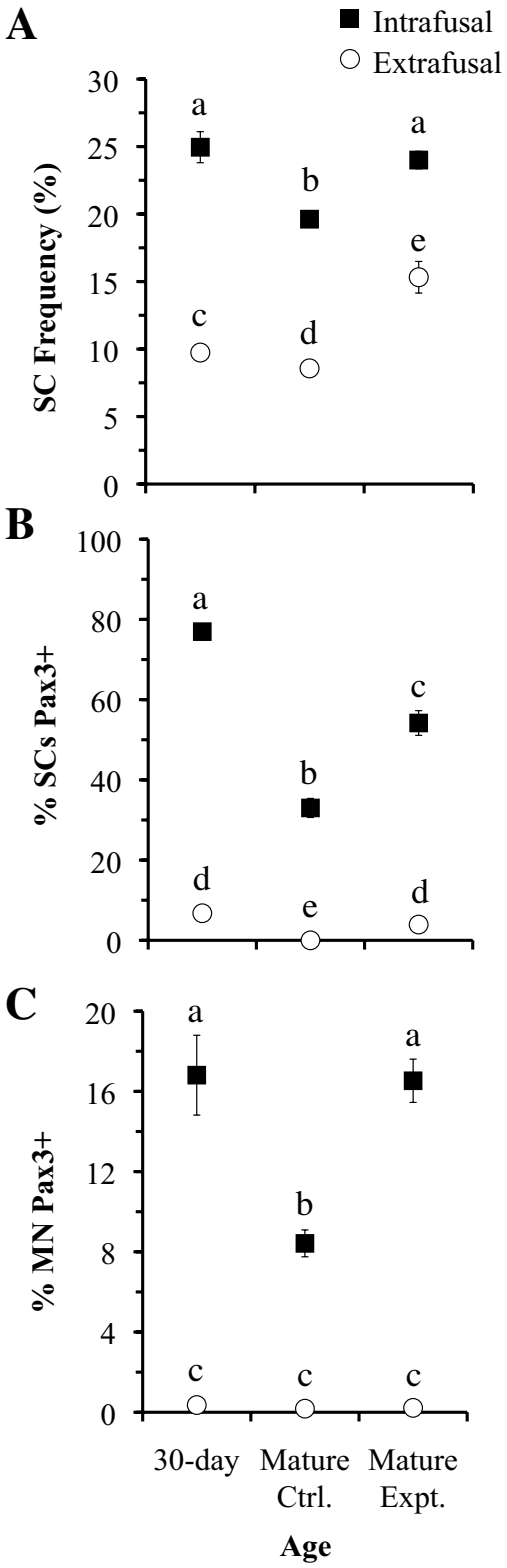
A
Intrafusal
Extrafusal
SC Frequency (%)
30
25
20
15
10
5
0
a
b
a
e
c
d
B
% SCs Pax3+
100
80
60
40
20
0
a
c
b
d
e
d
C
% MN Pax3+
20
16
12
8
4
0
a
a
b
c
c
c
30-day
Mature Ctrl.
Mature Expt.
Age

Figure 12 Posterior latissimus dorsi (PLD) muscle intrafusal and extrafusal nuclei data. Satellite cell (SC) frequency (A) is greater in intrafusal than extrafusal fiber profiles in each group studied and, in both intrafusal and extrafusal fiber profiles, is higher in experimentally overloaded (mature expt.) muscle than in mature control (ctrl.) muscle. Percentage of SCs expressing Pax3 (B) is always higher in intrafusal than extrafusal fiber profiles and, within both intrafusal and extrafusal fiber profiles, is greater with muscle overload versus mature control. Percentage of myonuclei (MN) expressing Pax3 (C) is always higher in intrafusal than extrafusal fiber profiles and, in intrafusal but not extrafusal fiber profiles, is greater with muscle overload versus control. Each parameter (SC Frequency, % SCs expressing Pax3, or % MN Pax3+) quantified, with the exception of % MN Pax3+ in extrafusal fiber profiles, decreases with aging from 30 to 145 (mature ctrl.) days. The values for each parameter of the overloaded mature muscle (mature expt.), with the exception of % MN Pax3+ in extrafusal fiber profiles, are more characteristic of those observed in less mature muscle (30-day). In each graph (A-C), symbols beneath the same lowercase letter are not significantly different ($p>0.05$) from one another. Symbols beneath different lowercase letters are significantly different ($p\leq0.05$) from one another. Each value is expressed as mean $\pm$ SE (n=5). Error bars that are not visible are smaller than the symbol used to denote each mean.

muscle overload (mature expt.) than either 30-day ($p<0.001$) or mature control ($p=0.006$) groups.

4.4.5 Satellite Cells Expressing Pax3

Mean percentage of Pax3-expressing SCs (%SCs Pax3+; Figure 12B) was always significantly ($p<0.001$) higher in intrafusal than extrafusal fiber profiles. In intrafusal fiber profiles, %SCs Pax3+ ranged from 73.33 to 83.33% in the 30-day group (average of 76.95 $\pm$ 1.71%), from 25.00 to 40.00% in the mature control group (mean of 33.00 $\pm$ 2.38%) and 45.45 to 63.64% in the mature experimental group (average of 54.18 $\pm$ 3.08%). In intrafusal fiber profiles, %SCs Pax3+ was significantly ($p<0.001$) higher in the 30-day group than in the mature control group. In the mature experimental group, the mean %SCs Pax3+ in intrafusal fiber profiles was significantly ($p=0.003$) greater than that of the mature control group, but significantly less ($p<0.001$) than the 30-day group. Within extrafusal fiber profiles, %SCs Pax3+ decreased significantly ($p<0.001$) from a mean of 6.75 $\pm$ 1.04% (varying from 3.45 to 9.09%) in the 30-day group, to zero in all five animals of the mature control group. Mean %SCs Pax3+ in extrafusal fiber profiles of the mature experimental group was 3.93 $\pm$ 0.47%, with a range of 2.99 to 5.48%. In extrafusal fiber profiles, %SCs Pax3+ in the mature experimental group was significantly ($p<0.001$) greater than the mature control group and statistically the same ($p=0.816$) as levels seen in the 30-day group.

4.4.6 Myonuclei Expressing Pax3

Mean percentage of Pax3-expressing MN (%MN Pax3+; Figure 12C) was higher in intrafusal than extrafusal fiber profiles in all three groups ($p<0.001$). Within intrafusal fiber profiles, %MN Pax3+ was higher in the 30-day group than the mature control group ($p<0.001$) with a range of 12.50 to 23.08% (mean of 16.81 $\pm$ 1.99%) and 6.45 to 10.64% (average of 8.42 $\pm$ 0.67%), respectively. With muscle overload, %MN Pax3+ was greater than the control group in mature animals ($p=0.003$) and equal to the 30-day group ($p=1.000$) with a range of 14.29 to 20.59% and mean of 16.53 $\pm$ 1.08%. The mean %MN Pax3+ in extrafusal fiber profiles was statistically equal in all three groups at less than 1% ($p=1.000$).

4.5 Discussion

This is the first study to show a change in the number of Pax3+ SCs in post-natal/post-hatch muscle as a result of experimental intervention. Functional muscle overload has been shown to produce a variety of changes within skeletal muscle on a gross, cellular and molecular level. Factors such as muscle wet weight (Gutmann *et al.* 1970; Baldwin *et al*. 1982; Roy *et al*. 1982), cell diameter (Roy *et al*. 1982), total muscle protein (Adams *et al.* 1999), growth factors (Adams *et al*. 1999), cell cycle markers and MRFs such as MyoD and myogenin (Adams *et al.* 1999; Ishido *et al.* 2004) are found to increase, while changes in contractile properties (Roy *et al*. 1982) and energy-generating enzyme patterns (Gutmann *et al*. 1970; Baldwin *et al*. 1982) also occur. Pax3 mRNA and protein have been shown to increase in rat plantaris during compensatory hypertrophy induced by surgical removal of the gastrocnemius (Hyatt *et al.* 2008). However, as muscle homogenates were analyzed in this rat model, the cellular location of the Pax3 was not demonstrated.

The function of Pax3 protein in mature muscle is unclear (Buckingham 2006; Relaix *et al.* 2006; Kuang and Rudnicki 2008). Pax3 has been previously shown to down-regulate before birth, after myogenesis is complete (Horst *et al.* 2006; Hutcheson *et al.* 2009). However, Pax3 has been located in SCs of a select group of mature muscles, including the mouse diaphragm and gracilis (Relaix *et al.* 2006). It is not known whether Pax3 in the SCs of mature muscle is a developmental vestige of embryonic myogenesis, and/or may be performing an active role. This study provides some insight into this question. Overload increased mean SC frequency within intrafusal fiber profiles by 22%. However, the mean number of Pax3+ SCs and Pax3+ MN in overloaded intrafusal fiber

profiles increased, respectively, by 64% and 96%. Thus, while overload increases the number of SCs, a greater proportion of the SCs and MN in overloaded muscle express Pax3. This suggests that Pax3 expression is associated with SC differentiation in overloaded muscle. If Pax3-expressing SCs were solely a developmental vestige, they would not likely show a disproportionate increase in number in response to muscle hypertrophy. Additional evidence is provided by analyses of extrafusal fibers. Experimental overload of mature PLD induces the reappearance of Pax3+ SCs, which were present in 30 day muscle but absent from the mature control PLD. This further supports the conclusion that Pax3 expression is not solely a rudiment of development, but rather is associated with SC differentiation in overloaded mature muscle.

This study concurs with the literature in that muscle overload via synergist tenotomy or ablation is an excellent model for inducing SC activation (Lowe and Alway 2002; Alway *et al.* 2005; Ishido *et al*. 2009). Increasing the load and subsequent strain on skeletal muscles initiates SC activation to repair the cellular damage (Hawke and Garry 2001). The precise role of Pax3 in this process is yet to be determined, but Pax3 is thought to be involved in the initial stages of SC activation and proliferation (Conboy and Rando 2002) and as a precursor to myogenic differentiation (Kuang and Rudnicki 2008). Developmentally, Pax3 is essential for the delamination and migration of myogenic precursors to the limb buds (Buckingham *et al.* 2003) and activates the c-Met receptor-encoding gene essential for myogenic cell migration (Bladt *et al.* 1995; Epstein *et al.* 1996). Pax3 lies upstream of MyoD and Myf5 (Maroto *et al.* 1997; Tajbakhsh *et al.* 1997), and the degradation of Pax3 is essential for the progression of myogenic

differentiation (Boutet *et al.* 2007). Therefore, the role of Pax3 in mature muscle may be one of cell migration or myogenic differentiation.

Pax3-expressing MN increase in numbers in intrafusal fiber profiles following muscle overload. Earlier in this thesis, novel Pax3 positive MN were shown to exist in intrafusal fiber profiles of muscle spindles and, to a lesser extent, in extrafusal fiber profiles making up the bulk of the ALD muscle (see Chapter 3). The increase in Pax3+ MN within intrafusal fiber profiles is undoubtedly associated with increases in SC frequency and Pax3+ SCs following muscle overload. As Pax3 lies upstream of MyoD and Myf5 (Maroto *et al.* 1997; Tajbakhsh *et al.* 1997; Relaix *et al*. 2006), Pax3+ MN may be in transition from SCs to MN. Pax3 may also have implications in cell movement, as Pax3 regulates the c-Met receptor critical for myogenic progenitor migration (Epstein *et al*. 1996; Keller *et al.* 2004). Pax3+ MN may be in the process of migrating from a satellite position on the surface of muscle fibers to a nuclear position within the fibers.

This study shows that mean extrafusal fiber diameter between overloaded and control muscles remains the same. However, the distribution of those fiber diameters changes under overloaded conditions. Greater numbers of relatively giant and tiny diameter extrafusal fibers exist in overloaded muscles compared to controls. This suggests that muscle fibers are growing both in diameter and length. The greater number of large diameter fibers indicate growth in fiber girth. Muscle fiber diameter has previously been shown to increase following compensatory overload in rat (Roy *et al.* 1982). The greater number of small diameter fibers may be accounted for by increases in the lengths of tapered fiber ends. Longitudinal growth occurs through the addition of

new sarcomeres to fiber ends (Griffin 1971; Williams and Goldspink 1971) and myoblasts are preferentially added to the ends of growing fibers (Zhang and McLennan 1995). As the tapered ends of fibers grow in length following muscle overload, a greater number of small diameter fiber profiles will be seen in a cross-section through the muscle. McClung *et al.* 2005 reported similar differences in fiber size distribution in functionally overloaded and nadrolone decanoate treated rat soleus muscle in which group means were statistically equal.

Intrafusal fiber size remains unchanged through normal post-hatch development of chicken ALD (see Chapter 3), and mouse extensor digitorum longus (Kozeka and Ontell 1981). In the current study, intrafusal fiber ellipse minor axis is the same at 30 days post-hatch as in mature control chicken PLD. Following muscle overload, however, intrafusal fiber size increases compared to control values. Muscle spindles constantly monitor length changes in skeletal muscle and intrafusal fibers frequently adjust their own lengths in tandem with the rest of the muscle (Dorward 1970; Vallbo 1974; Maier 1992). The overloaded PLD may elicit increased intrafusal fiber contraction, resulting in damage and subsequent repair. As new MN are added to repair damage, subsequent growth occurs, providing a possible explanation for the intrafusal fiber size increase. Maier *et al*. 1972 also reported an increase in intrafusal fiber size within overloaded cat medial gastrocnemius following denervation of its synergist muscles. Intrafusal fiber size has been shown to increase in the absence of afferent innervation (Kucera and Walro 1988). In the current study, afferent nerve stimulation may be altered following muscle overload, thereby disrupting the normal influence of sensory innervation on muscle fiber size.

Pax3 appears to function during SC activation in mature muscle. Muscle spindles may prove an excellent model for resolving the role(s) of Pax3, due to the high SC frequency and large numbers of SCs expressing Pax3 in intrafusal fiber profiles. Therapeutic advances in injury and disease management may be achieved through an increased understanding of Pax3 and general muscle maintenance in mature muscle (Kuang and Rudnicki 2008). Future studies utilizing the muscle spindle as an experimental model might explore the relationship among Pax3, cell proliferation, migration and MRF expression. As Pax3 has been postulated to play a role in SC activation and proliferation as well as myogenic differentiation, studies deciphering these interactions will be important in defining the role(s) of Pax3 within nuclei of mature muscle.

Chapter 5:

General Discussion

The findings of this study provide new insights into the expression and function of Pax3 in mature muscle. Pax3-expressing SCs are preferentially associated with intrafusal fibers of muscle spindles, as compared to the surrounding extrafusal fibers. This is true of both the ALD and PLD muscles, at each age studied. Muscle spindles constantly monitor length changes and adjust their own lengths in tandem with the surrounding muscle (Dorward 1970; Vallbo 1974; Maier 1992). This high level of activity may require amplification of normal cellular mechanisms for repairing regular wear and tear. Greater numbers of Pax3+ SCs in muscle spindles may aid in meeting the greater demands for repair and preservation of intrafusal fibers.

The relatively greater numbers of SCs expressing Pax3 within muscle spindles may also be related to the immature state of intrafusal muscle fibers. Higher SC frequency (Kirkpatrick *et al*. 2008), arrested growth (Kozeka and Ontell 1981), Myf5 expression (Zammit *et al*. 2004), and developmental myosin heavy chain expression (Walro and Kucera 1999; Liu *et al.* 2002) are all indicators of the relative immaturity of intrafusal fibers. As Pax3 is expressed in muscle precursor cells (Galli *et al.* 2008) and lies upstream of MyoD and Myf5 (Maroto *et al.* 1997; Tajbakhsh *et al.* 1997; Relaix *et al.* 2006), its greater expression in muscle spindles is in concert with an overall theme of immaturity.

Pax3 is not simply a remnant from early development. The expression of Pax3 within intrafusal fiber profiles, and to a lesser extent in adjacent extrafusal fiber profiles, can be disproportionately augmented by experimentally induced muscle hypertrophy. This indicates that Pax3 may play an active role in SC differentiation in mature muscle. Pax3 also regulates c-Met (Epstein *et al*. 1996; Keller *et al.* 2004), a receptor critical in

cell migration (Birchmeier and Brohmann 2000). Thus, Pax3 may aid in SC differentiation and migration from the surface of muscle fibers to nuclei within fibers.

The numbers of Pax3-expressing SCs in ALD and PLD decrease with maturation in both intrafusal and extrafusal fiber profiles. This parallels the general decrease in SC numbers observed during the maturation of both intrafusal and extrafusal fibers of these muscles (Kirkpatrick *et al.* 2008), and by studies of the extrafusal fibers of other muscles (Halevy *et al.* 2004; Shefer *et al.* 2006). A decrease in overall SC frequency and numbers with aging is correlated with a reduction in fiber regeneration and repair (Shefer *et al.* 2006; Brack and Rando *et al.* 2007). A decrease in the relative numbers of Pax3+ SCs within a declining SC population may further hinder the capacity of fibers for maintenance. This disproportionate decrease may also be indicative of an overall reduction in the activity of SCs, and provides additional evidence that Pax3 plays an active role in SC differentiation in mature muscle.

Slow contracting muscles, such as the ALD, generally function in maintaining posture and sustained locomotion, whereas fast-twitch muscles, such as the PLD, are activated in short sporadic bursts of strength (George and Berger 1966). Differences in SC frequency reflect the diverse functions of slow and fast muscles. SC frequency is greater in slow than fast contracting muscles, as confirmed in the current study, indicating a greater capacity or requirement for growth, regeneration and repair in slow contracting muscle (Schmalbruch and Hellhammer 1977; Gibson and Schultz 1983; Shefer *et al.* 2006; Kirkpatrick *et al.* 2008). Pax3 is expressed in a higher percentage of SCs within intrafusal and extrafusal fiber profiles of the fast PLD than the comparable fiber profiles of the slow ALD muscle at both 30 and 145 days post-hatch. Similarly,

Pax3-expressing MN are found more frequently in intrafusal fiber profiles of the PLD than ALD. Therefore, Pax3 expression does not appear to be correlated with the greater need for regenerative capacity and protein synthesis in slow contracting muscles as compared to fast contracting muscles. Pax3 is expressed in the SCs of some muscles but is absent or at lower numbers in SCs of other muscles, for no apparent reason (Relaix *et al.* 2006). This phenomenon may explain the different percentage of SCs expressing Pax3 in the ALD and PLD. The presence of Pax3 in SCs of mature muscle may be somewhat dependent upon the developmental ontogeny of the particular muscle.

Post-hatch expression of Pax3 in only a proportion of SCs in a select group of muscles brings up the possibility that Pax3+ SCs and Pax3- SCs come from different embryonic progenitor populations (Kuang and Rudnicki 2008). Evidence supporting this theory is the differential expression of Pax3 and Pax7 in the dermomyotome of somites. Pax3 expression is highest in the epaxial and hypaxial dermomyotome, while Pax7 expression is concentrated in the central dermomyotome (Galli *et al.* 2008). In addition, SCs of the trunk are thought to originate from central dermomyotome cells (Gros *et al*. 2005), while SCs of the limbs come from hypaxial dermomyotome (Schienda *et al.* 2006). Further characterization of Pax3 expression in SCs of post-hatch and post-natal muscle is needed to identify a possible link between the embryonic origins of SCs and adult expression of Pax3. However, new findings via genetic labeling suggest that all Pax7-expressing cells originate from Pax3+/Pax7- cells (Hutcheson *et al*. 2009), suggesting that all SCs may ultimately come from the same source.

Stem cell research has revealed potential treatments for numerous cases of physical trauma, degenerative conditions and genetic diseases. Included is the use of

stem cells for treatment of muscle disease or injury. Many stem cells are currently being studied in the context of potential muscle therapy, including interstitial muscle side population cells, muscle derived stem cells, bone marrow cells, circulating cells expressing CD133, pericytes, mesangioblasts and SCs (Endo 2007; Kuang and Rudnicki 2008). Donor cell choice, method of cell delivery, and factors affecting cell survival are important to decipher to maximize the regenerative potential of stem cells in muscle therapy. SC based therapy appears most promising because it amplifies the normal functions of SCs in muscle. SCs are also easily identifiable, accessible and plentiful in most muscles. Current challenges to SC based therapy include poor cell survival, self-renewal and migration after intramuscular injection (Boldrin and Morgan 2007; Kuang and Rudnicki 2008). The current study provides evidence for the role of Pax3 in SC activation, proliferation and/or migration in overloaded muscle. Thus, using Pax3-expressing SCs in muscle therapy may increase the efficiency of regeneration by increasing cell migration and self-renewal. SCs are highly heterogeneous in terms of expression of Myf5, MyoD, Pax3, etc., which may reflect a functional heterogeneity with respect to regenerative potential (Kuang and Rudnicki 2008). SC derived myoblasts lacking MyoD, for example, grafted with higher efficiency than MyoD+ cells after injection into injured mouse tibalis anterior (Asakura *et al.* 2007). Uncovering the optimal combination of myogenic factor expression is important to maximize the potential of SC in muscle regeneration. SC based therapy is also limited by the decreased myogenic potential of SCs after culture amplification (Boldrin and Morgan 2007; Kuang and Rudnicki 2008). This is also true for Pax3-expressing cells that have been isolated by flow cytometry from adult mouse diaphragm and used in grafting experiments

(Montarras *et al*. 2005). Optimizing culture conditions for SC myogenic potential will also be important to future SC based therapy.

A comprehensive understanding of the role of Pax3 in mature muscle is still lacking. Embryonic Pax3 knockout is lethal, so future studies must employ SC-specific deletion of Pax3 in mature muscle. Whether Pax3 is essential for SC function or acts to enhance any portion of that function remains to be answered. Mechanisms regulating the differential expression of Pax3 and its relationship to other myogenic factors in mature muscle must also be uncovered. It is important to develop a thorough understanding of the basic science behind Pax3 function and regulation in SCs before hastily turning attentions to clinical therapy and disease management. From both a science perspective and in the interest of human health, there are still far more questions than answers in this case and the focus should remain on the basics.

Literature Cited

Adams GR, Haddad F, Baldwin KM (1999) Time course of changes in markers of myogenesis in overloaded rat skeletal muscles. J Appl Physiol 87:1705-1712

Allouh MZ (2007) Satellite Cell and Myonuclear Distribution within Normal and Hypertrophic Models of Skeletal Muscle Growth, and the Expression of Myogenic Regulatory Factors during Growth. PhD Thesis. University of Saskatchewan

Allouh MZ, Yablonka-Reuveni Z, Rosser BWC (2008) Pax7 reveals a greater frequency and concentration of satellite cells at the ends of growing skeletal muscle fibers. J Histochem Cytochem 56:77-87

Alway SE (1993) Stretch induces nonuniform isomyosin expression in the quail anterior latissimus-dorsi muscle. Anat Rec 237:1-7

Alway SE, Siu PM, Murlasits Z, Butler DC (2005) Muscle hypertrophy models: Applications for research on aging. Can J Appl Physiol 99:1897-1904

Antonio J, Gonyea WJ (1993) Role of muscle fiber hypertrophy and hyperplasia in intermittently stretched avian muscle. J Appl Physiol 74:1893-1898

Antonio J, Gonyea WJ (1994) Muscle-fiber splitting in stretch-enlarged avian muscle. Med Sci Sports Exerc 26:973-977

Anderson JE (2000) A role for nitric oxide in muscle repair: nitric oxide-mediated activation of muscle satellite cells. Mol Biol Cell 11:1859-1874

Anderson JE (2006) The satellite cell as a companion in skeletal muscle plasticity: currency, conveyance, clue, connector and colander. J Exp Biol 209:2276-2292

Armstrong RB, Marum P, Tullson P, Saubert CW (1979) Acute hypertrophic response of skeletal-muscle to removal of synergists. J Appl Physiol 46:835-842

Asakura A, Hirai H, Kablar B, Morita S, Ishibashi J, Piras BA, Christ AJ, Verma M, Vineretsky KA, Rudnicki MA (2007) Increased survival of muscle stem cells lacking the *MyoD* gene after transplantation into regenerating skeletal muscle. Proc Natl Acad Sci USA 104:16552-16557

Baldwin KM, Valdez V, Herrick RE, MacIntosh AM, Roy RR (1982) Biochemical properties of overloaded fast-twitch skeletal-muscle. J Appl Physiol 52:467-472

Bandman E, Rosser BWC (2000) Evolutionary significance of myosin heavy chain heterogeneity in birds. Microsc Res Tech 50:473-491

Barker D, Hunt CC, McIntyre AK (1974) Muscle receptors. In Autrum H, Jung R, Loewenstein WR, MacKay DM, Teuber HL, eds. Handbook of Sensory Physiology, vol 3, no 2. Berlin, Springer-Verlag, 1-310

Birchmeier C, Brohmann H (2000) Genes that control the development of migrating muscle precursor cells. Curr Opin Cell Biol 12:725-730

Bladt F, Riethmacher D, Isenmann S, Aguzzi A, Birchmeier C (1995) Essential role for the *c-met* receptor in the migration of myogenic precursor cells into the limb bud. Nature 376:768-771

Boldrin L, Morgan JE (2007) Activating muscle stem cells: therapeutic potential in muscle diseases. Curr Opin Neurol 20:577-582

Botterman BR, Edgerton VR (1975) Histochemical profiles of rat soleus intrafusal fibres after chronic exercise. Histochem J 7:151-164

Boutet SC, Disatnik MH, Chan LS, Iori K, Rando TA (2007) Regulation of Pax3 by proteasomal degradation of monoubiquitinated protein in skeletal muscle progenitors. Cell 130:349-362

Brack AS, Rando TA (2007) Intrinsic changes and extrinsic influences of myogenic stem cell function during aging. Stem Cell Rev 3:226-237

Buckingham M (2006) Myogenic progenitor cells and skeletal myogenesis in vertebrates. Curr Opin Genet Dev 16:525-532

Buckingham M (2007) Skeletal muscle progenitor cells and the role of Pax genes. C R Biol 330:530-533

Buckingham M, Bajard L, Chang T, Daubas P, Hadchouel J, Meilhac S, Montarras D, Rocancourt D, Relaix F (2003) The formation of skeletal muscle: from somite to limb. J Anat 202:59-68

Buckingham M, Bajard L, Daubas P, Exner M, Lagha M, Relaix F, Rocancourt D (2006) Myogenic progenitor cells in the mouse embryo are marked by the expression of *Pax3/7* genes that regulate their survival and myogenic potential. Anat Embryol 211:S51-S56

Buckingham M, Relaix F (2007) The role of Pax genes in the development of tissues and organs: Pax3 and Pax7 regulate muscle progenitor cell functions. Annu Rev Cell Dev Biol 23:645-673

Camoretti-Mercado B, Dizon E, Jakovcic S, Zak R (1993) Differential expression of ventricular-like myosin heavy-chain messenger-RNA in developing and regenerating avain skeletal-muscles. Cell Mol Biol Res 39:425-437

Campion DR (1984) The muscle satellite cell: A review. Int Rev Cytol 87:225-251

Carson JA, Alway SE, Yamaguchi M (1995) Time-course of hypertrophic adaptions of the anterior latissimus-dorsi muscle to stretch overload in aged Japanese-quail. J Gerontol A Biol Sci Med Sci 50:B391-B398

Charge SBP, Rudnicki MA (2004) Cellular and molecular regulation of muscle regeneration. Physiol Rev 84:209-238

Chi N, Epstein JA (2002) Getting your Pax straight: Pax proteins in development and disease. Trends Genet 18:41-47

Coggeshall RE (1992) A consideration of neural counting methods. Trends Neurosci 15:9-13

Collins CA, Olsen I, Zammit PS, Heslop L, Petrie A, Partridge TA, Morgan JE (2005) Stem cell function, self-renewal, and behavioral heterogeneity of cells from the adult muscle satellite cell niche. Cell 122:289-301

Conboy IM, Rando TA (2002) The regulation of Notch signaling controls satellite cell activation and cell fate determination in postnatal myogenesis. Dev Cell 3:397-409

Day K, Shefer G, Richardson JB, Enikolopov G, Yablonka-Reuveni Z (2007) Nestin-GFP reporter expression defines the quiescent state of skeletal muscle satellite cells. Dev Biol 304:246-259

De Anda G, Rebollo MA (1967) The neuromuscular spindles in the adult chicken. I. Morphology. Acta Anat 67:437-451

Dorward PK (1970) Response characteristics of muscle afferents in the domestic duck. J Physiol 211:1-17

Dubowitz V, Sewry CA (2007) Muscle Biopsy: A Practical Approach, 3rd ed. Philadelphia, Elsevier, 83-84

Endo T (2007) Stem cells and plasticity of skeletal muscle cell differentiation: potential application to cell therapy for degenerative muscular diseases. Regenerative Med 2:243-256

Epstein JA, Shapiro DN, Cheng J, Lam PYP, Maas RL (1996) Pax3 modulates expression of the c-Met receptor during limb muscle development. Proc Natl Acad Sci USA 93:4213-4218

Estavillo J, Yellin H, Sasaki Y, Eldred E (1973) Observations on the expected decrease in proprioceptive discharge and purported advent of non-proprioceptive activity from the chronically tenotomized muscle. Brain Res 63:75-91

Galli LM, Knight SR, Barnes TL, Doak AK, Kadzik RS, Burrus LW (2008) Identification and characterization of subpopulations of Pax3 and Pax7 expressing cells in developing chick somites and limb buds. Dev Dyn 237:1862-1874

Gao LH, Kennedy JM (1992) Repression of the embryonic myosin heavy-chain phenotype in regenerating chicken slow muscle is dependent on innervation. Muscle Nerve 15:419-429

Gardahaut MF, Fontaineperus J, Rouaud T, Bandman E, Ferrand R (1992) Developmental modulation of myosin expression by thyroid-hormone in avain skeletal-muscle. Development 115:1121-1131

Gauthier GF, Orfanos G (1993) Developmental transitions in the myosin patterns of 2 fast muscles. J Muscle Res Cell Motil 14:99-109

George JC, Berger AJ (1966) Avian myology. New York, Academic Press

Gibson MC, Schultz E (1983) Age-related differences in absolute numbers of skeletal-muscle satellite cells. Muscle Nerve 6:574-580

Ginsborg BL (1960) Some properties of avian skeletal muscle fibres with multiple neuromuscular junctions. J Physiol 154:581-598

Glass DJ (2005) Skeletal muscle hypertrophy and atrophy signaling pathways. Int J Biochem Cell Biol 37:1974-1984

Gollnick PD, Parsons D, Riedy M, Moore RL (1983) Fiber number and size in overloaded chicken anterior latissimus dorsi muscle. J Appl Physiol 54:1292-1297

Gollnick PD, Timson BF, Moore RL, Riedy M (1981) Muscular enlargement and number of fibers in skeletal muscles of rats. J Appl Physiol 50:936-943

Goulding M, Lumsden A, Paquette AJ (1994) Regulation of Pax-3 expression in the dermomyotome and its role in muscle development. Development 120:957-971

Griffin GE, Williams PE, Goldspin G (1971) Region of longitudinal growth in striated muscle fibers. Nat New Biol 232:28-29

Gros J, Manceau M, Thome V, Marcelle C (2005) A common somatic origin for embryonic muscle progenitors and satellite cells. Nature 435:954-958

Gutmann E, Hajek I, Vitek V (1970) Compensatory hypertrophy of the latissimus dorsi posterior muscle by elimination of the latissimus dorsi anterior muscle of the chicken. Physiol Bohemoslov 19:483-489

Halevy O, Piestun Y, Allouh MZ, Rosser BWC, Rinkevich Y, Reshef R, Rozenboim I, Wleklinski-Lee M, Yablonka-Reuveni Z (2004) Pattern of Pax7 expression during myogenesis in the posthatch chicken establishes a model for satellite cell differentiation and renewal. Dev Dyn 231:489-502

Harvey AL, Marshal IG (1986) Muscle. In Sturkie PD, ed. Avian physiology, 4th ed. New York, Springer-Verlag, 74-86

Hawke TJ, Garry DJ (2001) Myogenic satellite cells: physiology to molecular biology. J Appl Physiol 91:534-551

Hikida RS, Wang RJ (1981) Tenotomy of the avian anterior latissimus dorsi muscle .1. Effect of age on fiber-type transformation and regeneration from the stump in chicks. Am J Anat 160:395-408

Horst D, Ustanina S, Sergi C, Mikuz G, Juergens H, Braun T, Vorobyov E (2006) Comparative expression analysis of Pax3 and Pax7 during mouse myogenesis. Int J Dev Biol 50:47-54

Hudson EH, Lanzillotti PJ (1955) Gross anatomy of the wing muscles in the family Corvidae. Am Midl Nat 53:1-44

Hutcheson DA, Zhao J, Merrell A, Haldar M, Kardon G (2009) Embryonic and fetal limb myogenic cells are derived from developmentally distinct progenitors and have different requirements for β-catenin. Genes Dev 23:997-1013

Hutton RS, Atwater SW (1992) Acute and chronic adaptations of muscle proprioceptors in response to increased use. Sports Med 14:406-421

Hyatt JPK, McCall GE, Kander EM, Zhong H, Roy RR, Huey KA (2008) Pax3/7 expression coincides with MyoD during chronic skeletal muscle overload. Muscle Nerve 38:861-866

Ishido M, Kami K, Masuhara M (2004) Localization of MyoD, myogenin and cell cycle regulatory factors in hypertrophying rat skeletal muscles. Acta Physiol Scand 180:281-289

Ishido M, Uda M, Kasuga N, Masuhara M (2009) The expression patterns of Pax7 in satellite cells during overload-induced rat adult skeletal muscle hypertrophy. Acta Physiol 195:459-469

Jin Z, Mannstrom P, Jarlebark L, Ulfendahl M (2007) Malformation of stria vascularis in the developing inner ear of the German waltzing guinea pig. Cell Tissue Res 328:257-270

Jirmanova I, Zelena J (1970) Effect of denervation and tenotomy on slow and fast muscles of the chicken. Z Zellforsch Mikrosk Anat 106:333-347

Kassar-Duchossoy L, Giacone E, Gayraud-Morel B, Jory A, Gomes D, Tajbakhsh S (2005) Pax3/Pax7 mark a novel population of primitive myogenic cells during development. Genes Dev 19:1426-1431

Kawakami A, Kimura-Kawakami M, Nomura T, Fujisawa H (1997) Distributions of PAX6 and PAX7 suggest their involvement in both early and late phases of chick brain development. Mech Dev 66:119-130

Keller C, Hansen MS, Coffin CM, Capecchi MR (2004) *Pax3:Fkhr* interferes with embryonic *Pax3* and *Pax7* function: implications for alveolar rhabdomyosarcoma cell of origin. Genes Dev 18:2608-2613

Kirkpatrick LJ, Allouh MZ, Nightingale CN, Devon HG, Yablonka-Reuveni Z, Rosser BWC (2008) Pax7 shows higher satellite cell frequencies and concentrations within intrafusal fibers of muscle spindles. J Histochem Cytochem 56:831-840

Kokkorogiannis T (2004) Somatic and intramuscular distribution of muscle spindles and their relation to muscular angiotypes. J Theor Biol 229:263-280

Kovacs CE, Meyers RA (2000) Anatomy and histology of flight muscles in a wing-propelled diving bird, the Atlantic puffin, *Fratercula arctica*. J Morphol 244:109-125

Kozeka K, Ontell M (1981) The 3-dimensional cytoachitecture of developing murine muscle spindles. Dev Biol 87:133-147

Kuang S, Rudnicki MA (2008) The emerging biology of satellite cells and their therapeutic potential. Trends Mol Med 14:82-91

Kucera J, Walro JM (1988) The effect of neonatal deafferentation or deefferentation on the immunocytochemistry of muscle spindles in the rat. Neurosci Lett 95:88-92

Lang D, Powell SK, Plummer RS, Young KP, Rugger BA (2007) PAX genes: Roles in development, pathophysiology, and cancer. Biochem Pharmacol 73:1-14

Lefeuvre B, Crossin F, Fontaine-Perus J, Bandman E, Gardahaut MF (1996) Innervation regulates myosin heavy chain isoform expression in developing skeletal muscle fibers. Mech Dev 58:115-127

Liu JX, Eriksson PO, Thornell LE, Pedrosa-Domellof F (2002) Myosin heavy chain composition of muscle spindles in human biceps brachii. J Histochem Cytochem 50:171-183

Lowe DA, Alway SE (2002) Animal models for inducing muscle hypertrophy: Are they relevant for clinical applications in humans? J Orthop Sports Phys Ther 32:36-43

Ludolph DC, Konieczny SF (1995) Transcription factor families: muscling in on the myogenic program. FASEB J 9:1595-1604

MacIntosh BR, Gardier PF, McComas AJ (2006) Skeletal muscle: form and function, 2nd ed. Windsor, Human Kinetics

Maier A (1992) The avian muscle spindle. Anat Embryol 186:1-25

Maier A, Eldred E, Edgerton VR (1972) The effect on spindles of muscle atrophy and hypertrophy. Exp Neurol 37:100-123

Margue CM, Bernasconi M, Barr FG, Schafer BW (2000) Transcriptional modulation of the anti-apoptotic protein BCL-XL by the paired box transcription factors PAX3 and PAX3/FKHR. Oncogene 19:2921-2929

Maroto M, Rashef R, Munsterberg AE, Koester S, Goulding M, Lassar AB (1997) Ectopic *Pax-3* activates *MyoD* and *Myf-5* expression in embryonic mesoderm and neural tissue. Cell 89:139-148

Matthews PBC (1964) Muscle spindles and their motor control. Physiol Rev 44:219-288

Matthews PBC (1981) Evolving views on the internal operation and functional role of the muscle spindle. J Physiol 320:1-30

Mauro A (1961) Satellite cell of skeletal muscle fibers. J Biophys Biochem Cytol 9:493-498

Maynard JA, Tipton CM (1971) The effect of exercise training and deneration on the morphology of intrafusal muscle fibers. Int Z Angew Physiol 30:1-9

McClung JM, Mehl KA, Thompson RW, Lowe LL, Carson JA (2005) Nandrolone decanoate modulates cell cycle regulation in functionally overloaded rat soleus muscle. Am J Physiol Regul Integr Comp Physiol 288:R1543-R1552

McCormick KM, Schultz E (1994) Role of satellite cells in altering myosin expression during avian skeletal-muscle hypertrophy. Dev Dyn 199:52-63

McDonagh MJN, Davies CTM (1984) Adaptive response of mammalian skeletal muscle to exercise with high loads. Eur J Appl Physiol 52:139-155

Meyers RA (1992) The morphological basis of folded-wing posture in the American kestrel (*Falco sparverius*). Anat Rec 232:493-494

Mitchell P, Steenstrup T, Hannon K (1999) Expression of fibroblast growth factor family during postnatal skeletal muscle hypertrophy. J Appl Physiol 86:313-319

Montarras D, Morgan J, Collins C, Relaix F, Zaffran S, Cumano A, Partridge T, Buckingham M (2005) Direct isolation of satellite cells for skeletal muscle regeneration. Science 309:2064-2067

Moore LA, Arrizubieta MJ, Tidyman WE, Herman LA, Bandman E (1992) Analysis of the chicken fast myosin heavy chain family. Localization of isoform-specific antibody epitopes and regions of divergence. J Mol Biol 225:1143-1151

O'Connor RS, Pavlath GK (2007) Point:Counterpoint: Satellite cell addition is/is not obligatory for skeletal muscle hypertrophy. J Appl Physiol 103:1099-1103

Ono Y, Iwamoto H, Takahara H (1993) The relationship between muscle growth and the growth of different fiber types in the chicken. Poult Sci 72:568-576

Otto A, Schmidt C, Patel K (2006) Pax3 and Pax7 expression and regulation in the avian embryo. Anat Embryol 211:293-310

Oustanina S, Hause G, Braun T (2004) Pax7 directs postnatal renewal and propagation of myogenic satellite cells but not their specification. EMBO J 23:3430-3439

Ovalle WK, Dow PR, Nahirney PC (1999) Structure, distribution and innervation of muscle spindles in avian fast and slow skeletal muscle. J Anat 194:381-394

Peter JB, Barnard RJ, Edgerton VR, Gillespie CA, Stempel KE (1972) Metabolic profiles of three fiber types of skeletal muscle in guinea pigs and rabbits. Biochemistry 11:2627-2633

Proske U (2006) Kinesthesia: The role of muscle receptors. Muscle Nerve 34:545-558

Raikow RJ (1985) Locomotor systems. In King AS, McLelland J, eds. Form and functions of birds, vol 3. New York, Academic Press, 57-146

Relaix F, Montarras D, Zaffran S, Gayraud-Morel B, Rocancourt D, Tajbakhish S, Mansouri A, Cumano A, Buckingham M (2006) Pax3 and Pax7 have distinct and overlapping functions in adult muscle porgenitor cells. J Cell Biol 172:91-102

Relaix F, Rocancourt D, Mansouri A, Buckingham M (2005) A Pax3/Pax7-dependent population of skeletal muscle progenitor cells. Nature 435:948-953

Rosales RL, Arimura K, Takenaga S, Osame M (1996) Extrafusal and intrafusal muscle effects in experimental botulinim toxin-A injection. Muscle Nerve 19:488-496

Rosser BWC, Farrar CM, Crellin NK, Andersen LB, Bandman E (2000) Repression of myosin isoforms in developing and denervated skeletal muscle fibers originates near motor endplates. Dev Dyn 217:50-61

Roy RR, Meadows ID, Baldwin KM, Edgerton VR (1982) Functional significance of compensatory overloaded rat fast muscle. J Appl Physiol 52:473-478

Rushbrook JI, Huang JM, Weiss C, Siconolfi-Baez L, Yao TT, Becker E, Feuerman M (1997) Characterization of the myosin heavy chains of avian adult fast muscles at the protein and mRNA levels. J Muscle Res Cell Motil 18:449-463

Sandri M (2008) Signaling in muscle atrophy and hypertrophy. Physiol 23:160-170

Schienda J, Engleka KA, Jun S, Hansen MS, Epstein JA, Tabin CJ, Kunkel LM, Kardon G (2006) Somitic origin of limb muscle satellite and side population cells. Proc Natl Acad Sci USA 103:945-950

Schmalbruch H, Hellhammer U (1977) The number of nuclei in adult rat muscles with special reference to satellite cells. Anat Rec 189:169-176

Schroder JM (1974) The fine structure of de- and reinnervated muscle spindles .1. The increase, atrophy and 'hypertrophy' of intrafusal muscle fibers. Acta Neuropath 30:109-128

Seale P, Sabourin LA, Girgis-Gabardo A, Mansouri A, Gruss P, Rudnicki MA (2000) Pax7 is required for the specification of myogenic satellite cells. Cell 102:777-786

Sewry CA, Dubowitz V (2001) Histochemistry and immunocytochemistry of muscle in health and disease. In Karpati G, Hilton-Jones D, Griggs RC, eds. Disorders of voluntary muscle, 7th ed. Cambridge University Press, 251-282

Shefer G, Van de Mark DP, Richardson JB, Yablonka-Reuveni Z (2006) Satellite-cell pool size does matter: defining the myogenic potency of aging skeletal muscle. Dev Biol 294:50-66

Shinin V, Gayraud-Morel B, Gomes D, Tajbakhsh S (2006) Asymmetric division and cosegregation of template DNA strands in adult muscle satellite cells. Nat Cell Biol 8:677-U69

Standring S, Ed. (2008) Gray's Anatomy – The Anatomical Basis of Clinical Practice, 40th ed. New York, Elsevier Churchill Livingstone, 103-117

Tajbakhsh S, Buckingham M (2000) The birth of muscle progenitor cells in the mouse: spatiotemporal considerations. Curr Top Dev Biol 48:225-268

Tajbakhsh S, Rocancourt D, Cossu G, Buckingham M (1997) Redefining the genetic hierarchies controlling skeletal myogenesis: *Pax-3* and *Myf-5* act upstream of *MyoD*. Cell 89:127-138

Tamaki T, Uchiyama S (1995) Absolute and relative growth of rat skeletal muscle. Physiol Behav 57:913-919

Taylor A, Ellaway PH, Durbaba R, Rawlinson S (2000) Distinctive patterns of static and dynamic gamma motor activity during locomotion in the decerebrate cat. J Physiol 529:825-836

Taylor A, Morgan DL, Gregory JE, Proske U (1994) The responses of secondary endings of cat soleus muscle spindles to succinyl choline. Exp Brain Res 100:58-66

Tidyman WE, Moore LA, Bandman E (1997) Expression of fast myosin heavy chain transcripts in developing and dystrophic chicken skeletal muscle. Dev Dyn 208:291-504

Timson BF (1990) Evaluation of animal-models for the study of exercise-induced muscle enlargement. J Appl Physiol 69:1935-1945

Tremblay P, Dietrich S, Mericskay M, Schubert FR, Li Z, Paulin D (1998) A crucial role for *Pax3* in the development of the hypaxial musculature and the long-range migration of muscle precursors. Dev Biol 203:49-61

Tzu J, Marinkovich MP (2008) Bridging structure with function: Structural, regulatory, and developmental role of laminins. Int J Biochem Cell Biol 40:199-214

Vallbo AB (1974) Afferent discharge from human muscle spindles in non-contracting muscles: steady state impulse frequency as a function of joint angle. Acta Physiol Scand 90:303-318

Vanden Berge JC, Zweers GA (1993) Myologia. In Baumel JJ, King AS, Breazille JE, Evan HE, Vanden Berge JC, eds. Handbook of avian anatomy: nomina anatomica avium. Cambridge, Publication of the Nuttall Ornithological Club, 189-247

van Emden, HF (2008) Statistics for Terrified Biologists. Malden, Blackwell Publishing, 40

Vater R, Cullen MJ, Harris JB (1994) The expression of vimentin in satellite cells of regenerating skeletal muscle *in vivo*. Histochem J 26:916-928

Venters SJ, Argent RE, Deegan FM, Perez-Baron G, Wong TS, Tidyman WE, Denetclaw WF, Marcelle C, Bronner-Fraser M, Ordahl CP (2004) Precocious terminal differeniation of pre-migratory limb muscle precursor cells requires positive-signalling. Dev Dyn 229:591-599

Walro JM, Kucera J (1999) Why adult mammalian intrafusal and extrafusal fibers contain different myosin heavy-chain isoforms. Trends Neurosci 22:180-184

Walro JM, Wang J, Story GM (1997) Afferent-inherent regulation of myosin heavy chain isoforms in rat muscle spindles. Muscle Nerve 20:1549-1560

Williams PE, Goldspink G (1971) Longitudinal growth of striated muscle fibres. J Cell Sci 9:751-767

Williams BA, Ordahl CP (2000) Fate restriction in limb muscle precursor cells precedes high-level expression of MyoD family member genes. Development 127:2523-2536

Winchester PK, Gonyea WJ (1992) A quantitative study of satellite cells and myonuclei in stretched avian slow tonic muscle. Anat Rec 232:369-377

Wozniak AC, Kong J, Bock E, Pilipowicz O, Anderson JA (2005) Signaling satellite-cell activation in skeletal muscle: markers, models, stretch, and potential alternate pathways. Muscle Nerve 31:283-300

Zammit PS, Carvajal JJ, Golding JP, Morgan JE, Summerbell D, Zolnerciks J, Partridge TA, Rigby PWJ, Beauchamp JR (2004) Myf5 expression in satellite cells and spindles in adult muscle is controlled by separate genetic elements. Dev Biol 273:454-465

Zammit PS, Partridge TA, Yablonka-Reuveni Z (2006) The skeletal muscle satellite cell: the stem cell that came in from the cold. J Histochem Cytochem 54:1177-1191

Zar, JH (1999) Biostatistical Analysis, 4th ed. Upper Saddle River, Prentice-Hall, 278-280

Zelena J, Soukup T (1993) Increase in the number of intrafusal muscle fibres in rat muscles after neonatal motor denervation. Neurosci 52:207-218

Zhang M, McLennan IS (1995) During secondary myotube formation, primary myotubes preferentially absorb new nuclei at their ends. Dev Dyn 204:168-177

Zhu Y, Fan X, Li X, Wu S, Zhang H, Yu L (2008) Effect of hindlimb unloading on resting intracellular calcium in intrafusal fibers and ramp-and-hold stretches evoked responsiveness of soleus muscle spindles in conscious rats. Neurosci Lett 442:169-173